AD-A198 698 NUMERICAL METHODS TO SOLVE THE PROBLEM OF SCATTERING 1/1
FROM ELECTRICALLY LA (U) ILLINOIS UNIV AT URBANA
COORDINATED SCIENCE LAB A CHANG ET AL AUG 88
UNCLASSIFIED UILU-ENG-88-2241 N00014-84-C-0149 F/G 17/9 NL

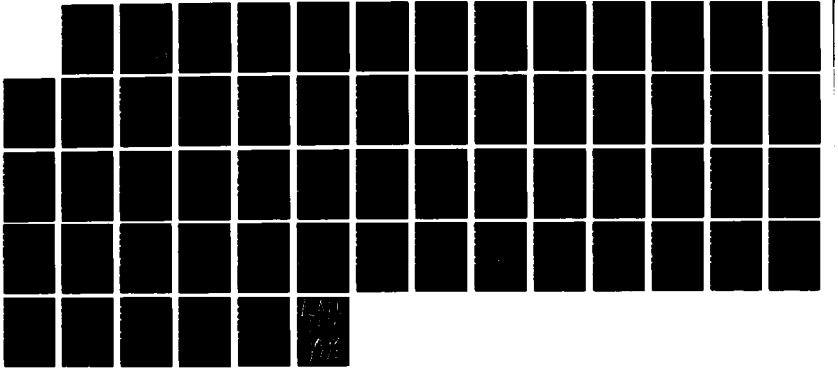

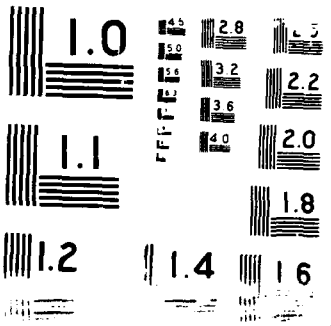
1.0
1.1
1.2
1.4
1.6
1.8
2.0
2.2
2.8
3.2
3.6
4.0
4.5
5.0
5.6

August 1988 UILU-ENG-88-2241

COORDINATED SCIENCE LABORATORY
College of Engineering

NUMERICAL METHODS TO SOLVE THE PROBLEM OF SCATTERING FROM ELECTRICALLY LARGE BODIES

A. Chang
R. Mittra

UNIVERSITY OF ILLINOIS AT URBANA-CHAMPAIGN

UNCLASSIFIED
SECURITY CLASSIFICATION OF THIS PAGE

REPORT DOCUMENTATION PAGE

1a. REPORT SECURITY CLASSIFICATION Unclassified	1b. RESTRICTIVE MARKINGS None
2a. SECURITY CLASSIFICATION AUTHORITY	3. DISTRIBUTION/AVAILABILITY OF REPORT Approved for public release; distribution unlimited
2b. DECLASSIFICATION/DOWNGRADING SCHEDULE	
4. PERFORMING ORGANIZATION REPORT NUMBER(S) UILU-ENG-88-2241	5. MONITORING ORGANIZATION REPORT NUMBER(S)
6a. NAME OF PERFORMING ORGANIZATION Coordinated Science Lab University of Illinois 6b. OFFICE SYMBOL (If applicable) N/A	7a. NAME OF MONITORING ORGANIZATION Office of Naval Research
6c. ADDRESS (City, State, and ZIP Code) 1101 W. Springfield Ave. Urbana, IL 61801	7b. ADDRESS (City, State, and ZIP Code) 800 N. Quincy St. Arlington, VA 22217
8a. NAME OF FUNDING/SPONSORING ORGANIZATION Joint Services Electronics Program 8b. OFFICE SYMBOL (If applicable)	9. PROCUREMENT INSTRUMENT IDENTIFICATION NUMBER N00014-84-C-0149
8c. ADDRESS (City, State, and ZIP Code) 800 N. Quincy St. Arlington, VA 22217	10. SOURCE OF FUNDING NUMBERS PROGRAM ELEMENT NO. / PROJECT NO. / TASK NO. / WORK UNIT ACCESSION NO

11. TITLE (Include Security Classification)
Numerical Methods to Solve the Problem of Scattering from Electrically Large Bodies.

12. PERSONAL AUTHOR(S)
Chang, A. and Mittra, R.

13a. TYPE OF REPORT	13b. TIME COVERED	14. DATE OF REPORT (Year, Month, Day)	15. PAGE COUNT
Technical	FROM _____ TO _____	1988 August	56

16. SUPPLEMENTARY NOTATION

17. COSATI CODES			18. SUBJECT TERMS (Continue on reverse if necessary and identify by block number)
FIELD	GROUP	SUB-GROUP	Electromagnetic scattering; iterative methods; radar cross section; and resistive strips.

19. ABSTRACT (Continue on reverse if necessary and identify by block number)

An alternative to directly inverting the large MoM matrix is to recast the problem in a form that is suitable for solution via iterative schemes. Although the use of iterative methods may enable one to treat scatterers that are an order of magnitude larger electrically, a close examination of them shows that most of them are not well-suited for handlin multiple excitations in an efficient manner. In this report some variational-iteration schemes based on the use of prechosen entire domain basis functions that are suitable not only for treating larger bodies but for handling miltiple incident angles as well are suggested. It is shown that, for this type of variational iteration schemes, the choice of an initial guess plays an important role in achieving a rapid convergence. Also, in an effort to further improve the convergence, a hybrid technique, where the method of moments is utilized to generate better gradient vectors in the iterative procedure, is developed. A simple case of scattering from a perfectly conducting or resistively-loaded strip is use to demonstrate the effectiveness of the methods.

20. DISTRIBUTION/AVAILABILITY OF ABSTRACT	21. ABSTRACT SECURITY CLASSIFICATION	
☒ UNCLASSIFIED/UNLIMITED ☐ SAME AS RPT. ☐ DTIC USERS	Unclassified	
22a. NAME OF RESPONSIBLE INDIVIDUAL	22b. TELEPHONE (Include Area Code)	22c. OFFICE SYMBOL

DD FORM 1473, 84 MAR — 83 APR edition may be used until exhausted. All other editions are obsolete.

SECURITY CLASSIFICATION OF THIS PAGE
UNCLASSIFIED

Numerical Methods to Solve the Problem of Scattering from Electrically Large Bodies

by

A. Chang and R. Mittra

ABSTRACT

An alternative to directly inverting the large MoM matrix is to recast the problem into a form that is suitable for solution via iterative schemes. Although the use of iterative methods may enable one to treat scatterers that are an order of magnitude larger electrically, a close examination of them shows that most of them are not well-suited for handling multiple excitations in an effiient manner. In this report some variational-iteration schemes based on the use of prechosen entire domain basis functions that are suitable not only for treating larger bodies but for handling miltiple incident angles as well are suggested. It is shown that , for this type of variational iteration schemes, the choice of an initial guess plays an important role in achieving a rapid convergence. Also, in an effort to further improve the convergence, a hybrid technique, where the method of moments is utilized to generate better gradient vectors in the iterative procedure, is developed. A simple case of scattering from a perfectly conducting or resistively-loaded strip is used to demonstrate the effectiveness of the methods.

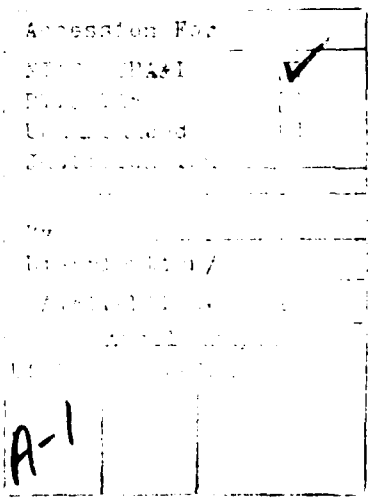

TABLE OF CONTENTS

1. INTRODUCTION

The conventional method of moments is not suitable for electrically large bodies due to the prohibitively large storage requirements in the computer. However, an alternative to directly inverting the MoM impedance matrix is to recast the problem in a manner such that iterative schemes can be employed to solve the problem of radar scattering from electrically large bodies. In this report, we examine a number of iterative techniques that appear to be useful for this purpose.

Although various types of iterative schemes for matirx equations, e.g., the conjugate gradient method, have been developed in the past, they were usually optimized to solve the problem for a single illuminating field (right-hand side) and, therefore, are not too well-suited for handling multiple incidences. However, since most of the applications require the computation of the radar cross section for a wide range of incident angles, it is important to be able to treat the multiple incidence case in an efficient manner. To this end, we suggest some variational-iteration schemes based on the use of prechosen, entire domain basis functions that not only enable one to treat larger bodies but allow the handling of multiple incident angles as well. The specific form of the basis functions chosen as an example in this chapter is the traveling-wave type. The advantages of using this type of basis functions are that their functional form is simple, known in advance and independent of the incident field. In this report, the problem of TM scattering from edge-loaded strips is investigated in detail to illustrate the use of different solution techniques mentioned above. Extensive numerical results are presented and some conclusions are drawn on the basis of these results. The case of TE scattering from edge-loaded strips is also discussed briefly.

2. ITERATIVE METHODS

2.1 Formulation for TM Scattering

The geometry of the edge-loaded strip and the coordinate system used is shown in Figure 2.1 for TM scattering. On the strip, the incident plane wave is given by

$$\mathbf{E}^{in}(x) = \mathbf{z}\, e^{jk_o x\cos\theta_o} \tag{2.1}$$

where θ_o is the incident angle measured from the positive x-axis. The general three-dimensional integral equation for a thin resistive scatterer has the form

$$\mathbf{E}^{in}_{tan}(\mathbf{r}) = R(\mathbf{r})\, \mathbf{J}(\mathbf{r}) - \mathbf{E}^{s}_{tan}(\mathbf{r}) \qquad \mathbf{r} \text{ on the surface S} \tag{2.2}$$

where

$$\mathbf{E}^{s} = -j\omega\mathbf{A} - \nabla\phi \tag{2.3}$$

$$\mathbf{A}(\mathbf{r}) = \mu\int_S \mathbf{J}(\mathbf{r}')G(\mathbf{r},\mathbf{r}')\, d\mathbf{r}' \tag{2.4}$$

$$\phi(\mathbf{r}) = \frac{1}{j\omega\varepsilon}\int_S \nabla'\cdot\mathbf{J}(\mathbf{r}')G(\mathbf{r},\mathbf{r}')\, d\mathbf{r}' \tag{2.5}$$

where S denotes the surface of the scatterer. Specialized to an infinitely thin resistive strip with the incident electric field in TM polarization, it becomes

$$E^{in}(x) = R(x)\, J(x) - E^{s}(x) \qquad \text{on the strip} \tag{2.6}$$

where

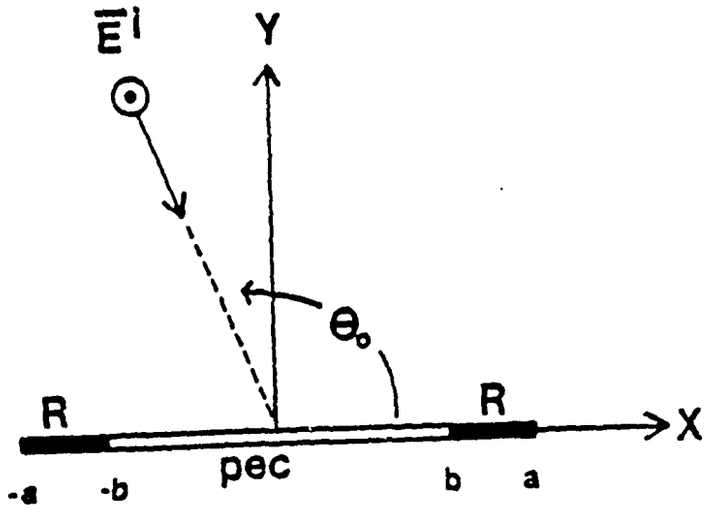

Figure 2.1 Geometry of the edge-loaded strip for TM scattering.

$$E^s(x) = -jk_o\eta \int_{-a}^{a} J(x')\, G(x,x')\, dx' \tag{2.7}$$

$$G(x,x') = \frac{1}{4j} H_o^{(2)}(k_o|x-x'|) \tag{2.8}$$

$$G(\alpha) = \frac{1}{2j\sqrt{k_o^2-\alpha^2}} \tag{2.9}$$

and k_o denotes the free-space wave number, η is the intrinsic impedance of the free space, and α is the Fourier transform (spectral) variable. In the above equations, $G(x,x')$ is the two-dimensional Green's function, $E^s(x)$ denotes the scattered field, and the quantities in italics indicate the Fourier transforms with α as the transform variable. Equation (2.6) is the electric field integral equation (EFIE) for the problem of TM scattering from a resistively edge-loaded strip. The convolution integral for the scattered field, given in Eq. (2.7), can be efficiently computed using the Fast Fourier Transform (FFT). In the following sections, various ways of solving the EFIE in Eq. (2.6) are investigated in detail.

2.2 Conjugate Gradient Method (CGM)

The conjugate gradient method is based on the conjugate direction method and includes an algorithm for the generation of mutually conjugate p-functions [1]. It has been applied to different types of electromagnetic scattering problems in the past [2], [3], [4], [5]. In general, the conjugate gradient method converges quite rapidly for a matrix whose eigenvalue spectrum is such that a large number of its eigenvalues are bunched closely together. This usually happens for diagonally dominant matrices [6]. For the particular problem of TM scattering from an edge-loaded strip, CGM works well for any single incidence and gives accurate results in a few iterations. However, CGM is not the most suitable approach when one desires to solve the problem for many incident angles simultaneously, because one must start anew and generate an entire sequence of expansion functions (gradient vectors) each time a new incident field is inserted into the integral equation such

as Eq. (2.6). Since CGM generates a sequence of the orthogonal gradients which span the entire space, one might conjecture that a set of gradient vectors generated for one incident angle could be used for all of the other incident fields and, consequently, the generation of a new set of gradient vectors would not be required each time the angle of illumination is changed. In practice, however, the numerically-generated expansion functions quickly lose their orthogonality because of computer round-off error and it is totally impractical to use the same functions even for moderately separated angles of incidence. Since CGM is numerically rigorous and barring a build-up of round-off errors, it generates the same solution as would be obtained via the matrix method in the context of MoM, it is used to check the convergence of other iterative algorithms presented below. However, a detailed study of the application of CGM and its variations to different types of electromagnetic field problems is beyond the scope of this report and the reader is referred to [7], [8] for additional information.

2.3 Variational Iteration

In this section, we describe iterative algorithms for simultaneous treatment of multiple incident angles. We begin with a set of prechosen expansion functions which give equal weight to all incident angles. Next, we devise an iterative algorithm for minimizing an error functional which is a measure of the satisfaction of the boundary condition on the strip. Prechoosing the direction vectors (expansion functions) obviates the need for generating them repeatedly for different incident angles, as is done in CGM. In this section, the expansion functions are chosen to be the plane-wave type although one could just as easily choose them differently, if one so desired. After the iteration is carried out, the current is expressed in the form

$$J(x) = J_o(x) + \sum_{n=1}^{N} \eta_n \, e^{jk_o x \cos\theta_n} \tag{2.10}$$

where k_o is the free-space wave number, θ_n is the angle measured from the positive x-axis, $J_o(x)$ is an initial guess, and η_n is the complex weighting coefficient generated in a manner to be explained below. Once these weighting coefficients are determined, we have the traveling-wave representation of the induced current on the strip. There are two advantages to using plane-wave-type basis functions. First, their functional form is very simple and, consequently, they can be computed easily and inexpensively. Second, since the current is already expressed in terms of traveling waves, it is a straightforward matter to identify which traveling-wave component has the dominant contribution to the far field for a given angle of observation. To illustrate this point, suppose we start with zero as the initial guess of the current on the strip. Then we have

$$J(x) = \sum_{n=1}^{N} \eta_n \, e^{jk_o x \cos\theta_n} \tag{2.11}$$

The scattered field in the far zone can be found by using the asymptotic expression for the Hankel function [9] and can be written as

$$E^s(\theta) = -\frac{k_o \eta \, e^{-j\left(k_o\rho+\frac{3\pi}{4}\right)}}{\sqrt{8\pi k_o \rho}} \int_{-a}^{a} J(x') \, e^{jk_o x' \cos\theta} \, dx'$$

$$= -\frac{2k_o \eta \, a \, e^{-j\left(k_o\rho+\frac{3\pi}{4}\right)}}{\sqrt{8\pi k_o \rho}} \sum_{n=1}^{N} \eta_n \frac{\sin[k_o a(\cos\theta+\cos\theta_n)]}{k_o a(\cos\theta+\cos\theta_n)} \tag{2.12}$$

Equation (2.12) shows that the far field is a combination of sinc functions, i.e., sinx/x type functions. These functions peak at different angles, given by $(\pi-\theta_o)$, where the argument of the sinc function becomes zero Note that, in a method such as CGM, it may be quite difficult to extract different traveling-wave components from the final induced current obtained. We also observe that when the basis functions are prechosen, i.e., they are not generated via the iteration

algorithm, the same set of basis functions can be employed for an arbitrary incident angle. Although this kind of generality in the method is a very desirable characteristic, it should be pointed out that the accuracy we obtain for each incident angle may not be as good as that obtained by CGM or any other single-incidence oriented algorithm. However, as has already been noted before, these single-incidence oriented algorithms generate gradient vectors that are optimal only for a particular incident angle, and, consequently, are ill-suited for the treatment of multiple incident angles. In contrast, the use of an iterative algorithm with prechosen basis functions allows one to treat multiple incident angles simultaneously with the same set of basis functions. The conventional method of moments may also be employed effectively if the matrix size is not too large. The purpose of developing an iterative procedure is to circumvent the problem of large matrices which cannot be conveniently treated by the direct inversion method and to exploit any symmetry or sparseness that arises due to the nature of the problem under consideration.

2.3.1 Minimization of the boundary condition error

In this section, an algorithm for variational iteration with the second minimization step (SMS), minimizing $| y - Lx_a |^2$, is derived, where y is the incident field, x_a is an approximate solution, and L is the integral operator. The derivation of SMS for this particular type of functional has been given in [5] and will not be repeated here. The resultant expressions are summarized below.

Suppose we are given a set of basis functions g_1 through g_N and an integral equation of the form

$$L x_{ex} = y \tag{2.13}$$

where x_{ex} is the unknown to be determined. As the result of minimizing the functional on the boundary condition error, the weighting coefficients for these basis functions are given by

$$\eta_n = \frac{< F_{n-1}, \bar{f}_n >}{< \bar{f}_n, \bar{f}_n >} \tag{2.14}$$

where

$$F_{n-1} = y - L\, x_{n-1}$$

$$f_n = L\, g_n$$

$$\bar{g}_n = g_n - \xi_n \bar{g}_{n-1} \tag{2.15}$$

$$f_n = f_n - \xi_n f_{n-1}$$

$$\xi_n = \frac{< \bar{f}_{n-1}, f_n >}{< \bar{f}_{n-1}, \bar{f}_{n-1} >}$$

where g_n's are the predetermined basis functions, while g_n's with the bar on top denote the modified g_n's obtained via the second minimization step (SMS). The inner product is defined as

$$< f, g > = \int_D f \cdot g^* \, dx \tag{2.16}$$

where D is the domain of the given problem and "*" denotes the complex conjugate.

2.3.2 Minimization of the error on the induced current

The convergence of the iterative algorithm minimizing the boundary condition error, as described in Section 2.3.1, does not always guarantee the convergence of the approximate solution

to the true one. It has been noted in the past that situations exist where, although the boundary condition error is reduced below the prescribed level, the computed solution is not close to the true solution. In this section an algorithm for variational iteration with the second minimization step, which directly minimizes the error on the solution itself, i.e., $| x_{ex} - x_a |^2$, is derived, where x_{ex} denotes the exact solution to the problem under consideration and x_a an approximate solution which is generated in a suitable manner. The minimization of the error on the current is achieved by utilizing the adjoint operator, L^A. Since we do not know the exact solution, x_{ex} , to the problem, we cannot explicitly calculate the quantity $| x_{ex} - x_a |^2$. However, it is still possible to minimize the functional $| x_{ex} - x_a |^2$. Since the derivation for SMS minimizing this functional is quite different from that given in Section 2.3.1, where the boundary condition error is minimized, we show below the steps involved in detail.

Suppose that we have already iterated up to the $(n-1)^{th}$ step. Then we have

$$F_{n-1} = x_{ex} - x_{n-1} \tag{2.17}$$

$$ERR_{n-1} = < F_{n-1}, F_{n-1} > = < x_{ex} - x_{n-1}, \; x_{ex} - x_{n-1} > \tag{2.18}$$

where F_n denotes the residual on the current and ERR_n the value of the error evaluated at the n^{th} step. For the problem of TM scattering from the edge-loaded strip, the adjoint operator is known and is given by

$$L^A(\cdot) = R(x) \, (\cdot) - \int_D (\cdot) \, G^*(x,x') \, dx' \tag{2.19}$$

where "*" means the complex conjugate of the quantity. Let the expansion functions Ψ_n be the plane-wave functions, i.e.,

$$\psi_n = e^{jk_o x\cos\theta_n} \tag{2.20}$$

Defining the n^{th} gradient vector g_n to be

$$g_n = L^A\psi_n \tag{2.21}$$

we can write

$$x_n = x_{n-1} + \eta_n g_n \tag{2.22}$$

$$F_n = F_{n-1} - \eta_n g_n$$

Then the error on the current at the n^{th} step is given by

$$ERR_n = < F_n, F_n > \tag{2.23}$$

$$= < F_{n-1}, F_{n-1} > - \eta_n < g_n, F_{n-1} > - \eta_n^* < F_{n-1}, g_n > + |\eta_n|^2 < g_n, g_n >$$

Minimizing this error (first minimization step), we obtain the weighting coefficient for the n^{th} gradient, which is given by

$$\eta_n = \frac{< F_{n-1}, g_n >}{< g_n, g_n >} \tag{2.24}$$

The numerator in the above expression can be written as

$$< F_{n-1}, g_n > = < x_{ex} - x_{n-1}, g_n > = < x_{ex}, g_n > - < x_{n-1}, g_n > \tag{2.25}$$

Notice that $< x_{n-1}, g_n >$ is known since x_{n-1} and g_n are known. Also

$$< x_{ex}, g_n > = < x_{ex}, L^A \psi_n > = < Lx_{ex}, \psi_n > = < y, \psi_n > \tag{2.26}$$

Therefore, we can write

$$\eta_n = \frac{< F_{n-1}, g_n >}{< g_n, g_n >} = \frac{< y, \psi_n > - < x_{n-1}, L^A \psi_n >}{< L^A \psi_n, L^A \psi_n >} \tag{2.27}$$

All the terms appearing in the above expression for η_n are known. Having found the weighting coefficient η_n, we can rewrite the error given in Eq. (2.23) in the following manner. For the convenience of notation, let

$$A_n = < F_{n-1}, g_n > = < y - Lx_{n-1}, \psi_n > \tag{2.28}$$

$$B_n = < g_n, g_n >$$

where the current expansion functions, g_n's, are given by Eq. (2.21). Then the error on the current is given by

$$ERR_n = < F_{n-1}, F_{n-1} > - \frac{| A_n |^2}{B_n} \tag{2.29}$$

The second minimization step aims at maximizing the second term in Eq. (2.29), thereby obtaining the greatest reduction possible in the error. One way of achieving such maximization is to define a new gradient

$$\bar{g}_n = g_n - \xi_n g_{n-1} \tag{2.30}$$

where ξ_n is the unknown weighting coefficient to be determined as the result of the second minimization step. Since we can write the residual as

$$F_n = x_{ex} - x_n = F_{n-1} - \eta_n g_n = F_{n-1} - \frac{< F_{n-1}, g_n >}{< g_n , g_n >} g_n \tag{2.31}$$

we have

$$< F_n, g_n > = < F_{n-1}, g_n > - \frac{< F_{n-1}, g_n >}{< g_n, g_n >} < g_n, g_n > \tag{2.32}$$

$$= < F_{n-1}, g_n > - < F_{n-1}, g_n > = 0$$

Notice that the numerator of the second term in Eq. (2.29) remains the same, i.e.,

$$\bar{A}_n = < F_{n-1}, g_n - \xi_n g_{n-1} >$$

$$= < F_{n-1}, g_n > - \xi_n < F_{n-1}, g_{n-1} > = < F_{n-1}, g_n > = A_n \tag{2.33}$$

The modified denominator is given by

$$\bar{B}_n = < \bar{g}_n, \bar{g}_n > \tag{2.34}$$

$$= < g_n, g_n > - \xi_n < g_{n-1}, g_n > - \xi_n^* < g_n, g_{n-1} > + | \xi_n |^2 < g_{n-1}, g_{n-1} >$$

Since the numerator remains the same, the maximization of the second term in Eq. (2.29) is achieved by minimizing the denominator. Upon carrying out this minimization, we obtain the following expression for the unknown weighting coefficient ξ_n :

$$\xi_n = \frac{< g_n - g_{n-1} >}{< g_{n-1}, g_{n-1} >} \tag{2.35}$$

Inserting Eq. (2.35) into Eq. (2.34), we finally obtain

$$\bar{B}_n = B_n - \frac{| < g_n, g_{n-1} > |^2}{B_{n-1}} \tag{2.36}$$

This completes the implementation of the variational-iteration procedure for minimizing the residual on the current. As has been noted before, the error on the current itself cannot be computed explicitly since we do not have access to the true solution. Thus, to check the convergence of the iteration procedure, the functional form of the approximate current at each step of the iteration is substituted into the expression for the error on the boundary condition, and this error is used as a measure of the accuracy of the solution for the current.

2.3.3 Numerical results

Figures 2.2, 2.3 and 2.4 show the bistatic radar cross sections obtained for three different incident angles by the variational-iteration methods described above and they are compared to those computed from CGM. The strip width is 2 λ and is edge-loaded with the maximum resistivity of 200 ohms at the edges of the strip and tapered in a linear fashion to zero resistivity at 0.41 λ from each edge. In the variational iteration, the same set of nine plane-wave-type basis functions is used as the prechosen gradient vectors for all three incident angles. As can be seen in the figures, two

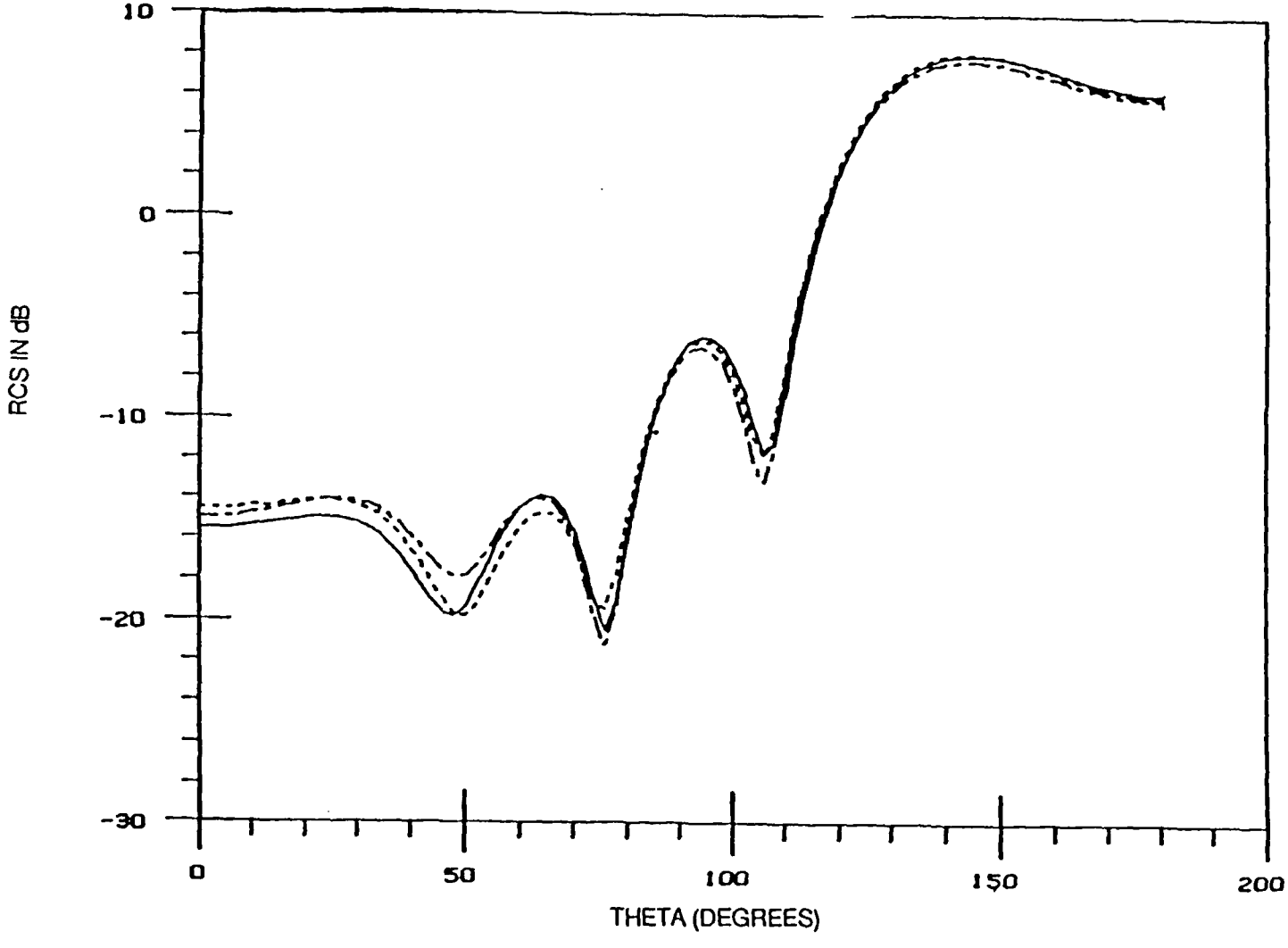

Figure 2.2 Bistatic RCS for 30 degree incidence.
Solid line --- CGM.
Dotted line -- Minimizing the boundary condition error.
Other --- Minimizing the error on the current.

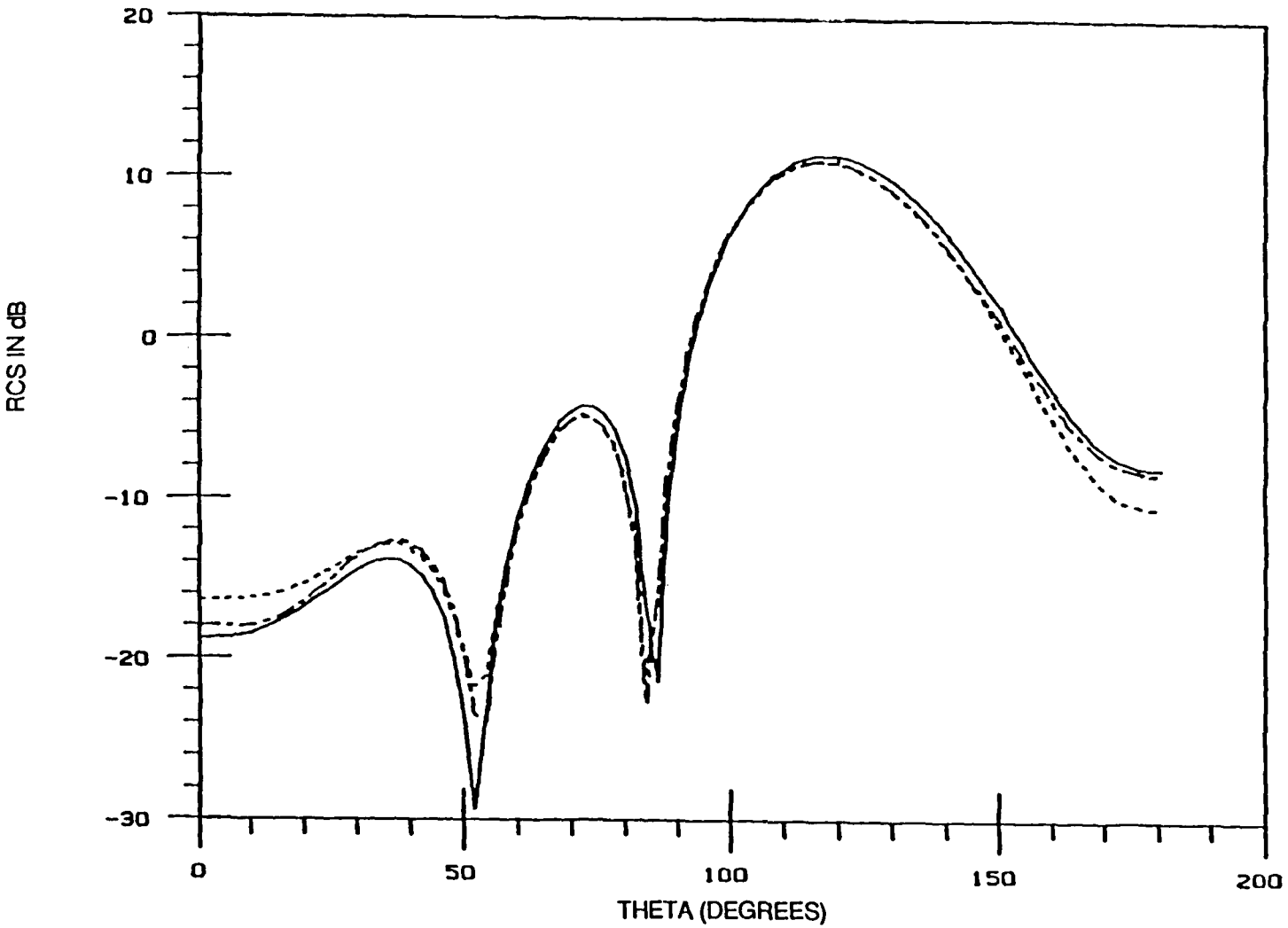

Figure 2.3 Bistatic RCS for 60 degree incidence.
Solid line --- CGM.
Dotted line -- Minimizing the boundary condition error.
Other --- Minimizing the error on the current.

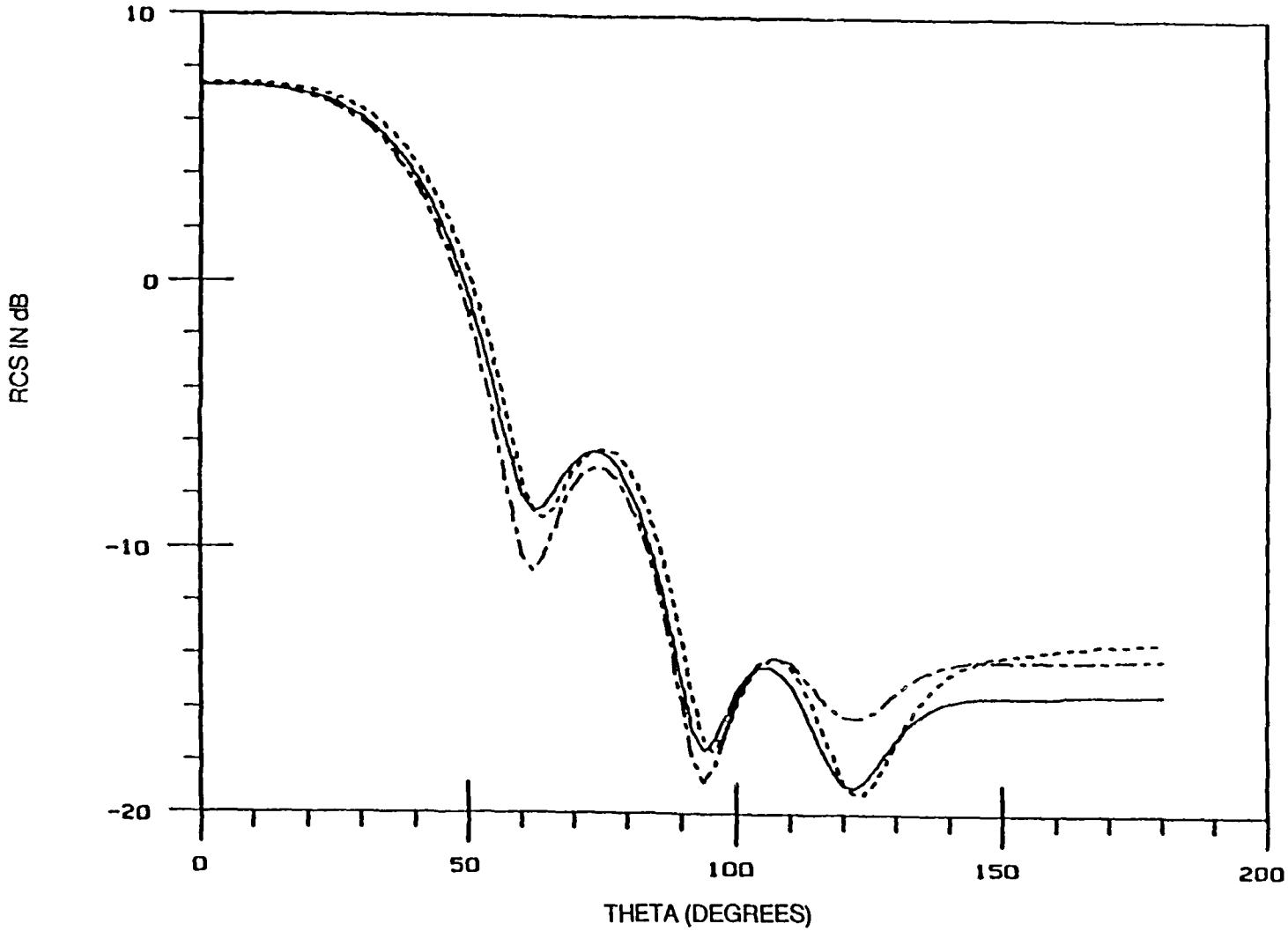

Figure 2.4 Bistatic RCS for 180 degree (grazing) incidence.
Solid line --- CGM.
Dotted line -- Minimizing the boundary condition error.
Other --- Minimizing the error on the current.

variational iteration schemes described in Sections 2.3.1 and 2.3.2 seem to yield about the same results for the particular problem of TM scattering from edge-loaded strips, in terms of accuracy and convergence.

2.4 Preconditioning in the Spectral Domain

Preconditioning of a matrix equation

$$A\,x = b \tag{2.37}$$

where A is the matrix operator, b the excitation vector, and x the unknown, usually consists of finding a pair of matrices P and Q and transforming the original equation into an equivalent pair of equations

$$PAQy = Pb \tag{2.38}$$

$$x = Qy \tag{2.39}$$

If the matrices P and Q are chosen such that the condition number of PAQ is smaller than that of A, an iterative algorithm such as CGM will generally converge faster on the preconditioned system than on the original system [10], [11]. In this section, a simple way of preconditioning an integral equation in the spectral domain is introduced. The advantage of doing the preconditioning in the spectral domain is that the operation involved is a simple algebraic multiplication or division rather than matrix multiplication or matrix inversion. The integral equation in the space domain is given by

$$R(x)\,J(x) - \int_S J(x')\,G_p(x,x')\,dx' = y(x) \tag{2.40}$$

on the strip, where G_p is the modified Green's function, which is simply the original Green's function multiplied by an appropriate scale factor. Let H be a preconditioning operator in the spectral domain. Fourier transforming the above integral equation, multiplying both sides of the transformed equation by H and inverse Fourier transforming the resultant equation yield the preconditioned version of Eq. (2.40). The preconditioned operator equation can be written as

$$\theta F^{-1} < H\, F[\theta R(x)\, J(x)] > - \theta F^{-1} < H\, F[\theta F^{-1}(JG_p)] > = \theta F^{-1} < HF[\theta y] > \qquad (2.41)$$

where θ is a truncation factor which is set to 1 if on the strip and 0 otherwise. F denotes the forward Fourier transform and F^{-1} the inverse Fourier transform. The idea is to choose H such that the preconditioned operator will approximate an identity operator. If the strip is perfectly conducting, then choosing the preconditioning operator H to be the inverse of G_p guarantees the preconditioned operator to be an approximate identity operator, and an iterative algorithm applied to this preconditioned equation converges very rapidly. However, if the strip is edge loaded, it can be shown that there is no general way of finding the operator H that will lead to an approximate identity operator after preconditioning. Also, it is noted that when the operator is preconditioned in the manner described in Eq. (2.41), the use of prechosen gradient vectors, such as plane-wave-type functions, yields poor results. To have reasonable results with this type of preconditioning, it is necessary to choose the gradients that are closely related to the residual F_{n-1}, which, in turn, is intimately related to the incident angle. Therefore, as in the case of CGM, this type of preconditioning in the spectral domain may not be suitable to treat multiple incident angles.

Some of the results for a 4.5 λ wide PEC strip obtained by the preconditioning technique described above are shown in Figures 2.5, 2.6, 2.7 and 2.8. Preconditioning is done with the inverse of G_p as the preconditioning operator. The current expansion functions are chosen to be the residuals, F_{n-1}'s. When the strip is perfectly conducting, preconditioning in this manner gives faster convergence than CGM. However, as R_{max} increases, the number of iterations needed to achieve the same order of accuracy as that given by CGM also increases.

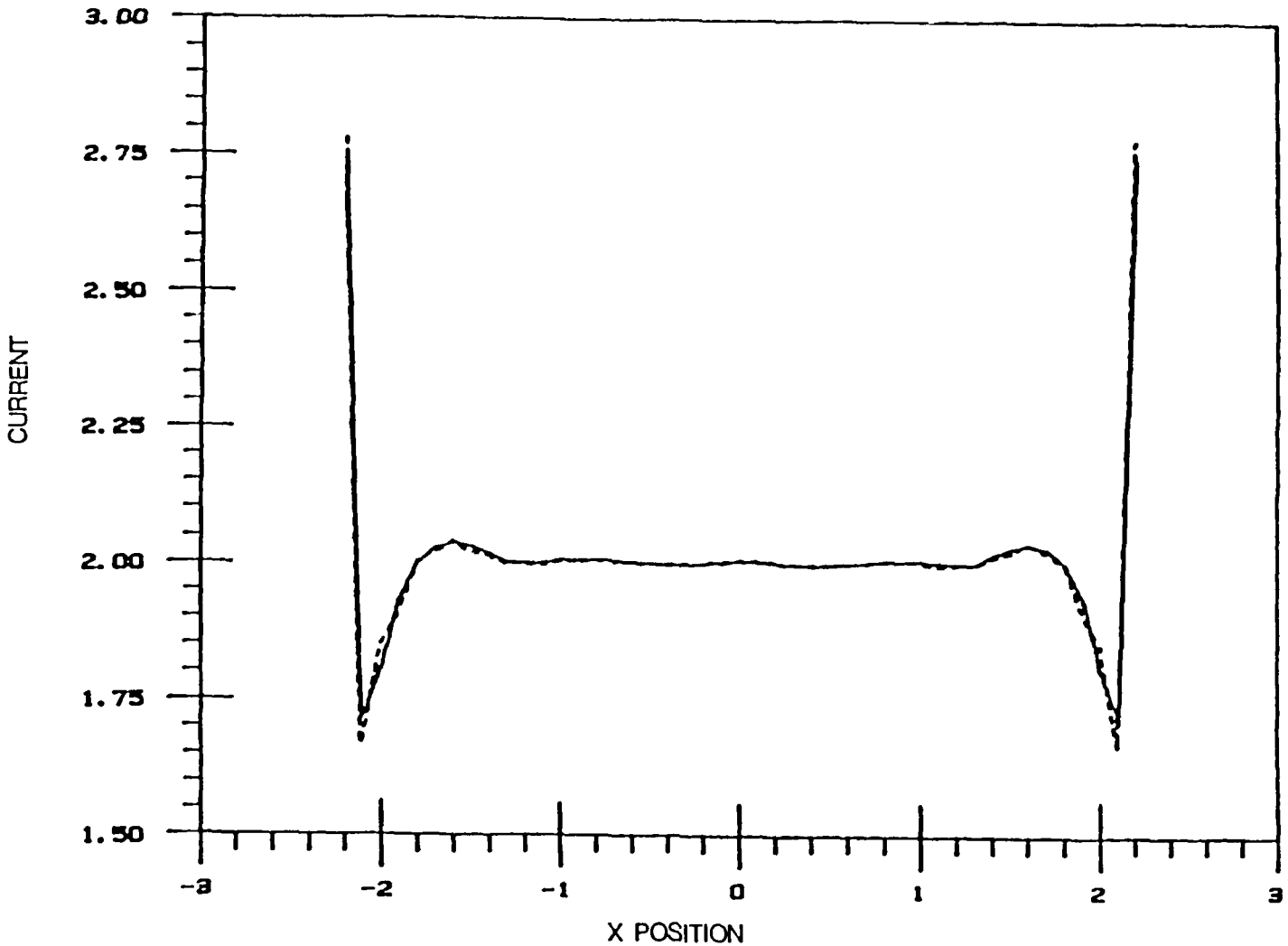

Figure 2.5 Magnitude of the induced current for normal incidence.
Solid line --- CGM.
Dotted line -- Preconditioning.

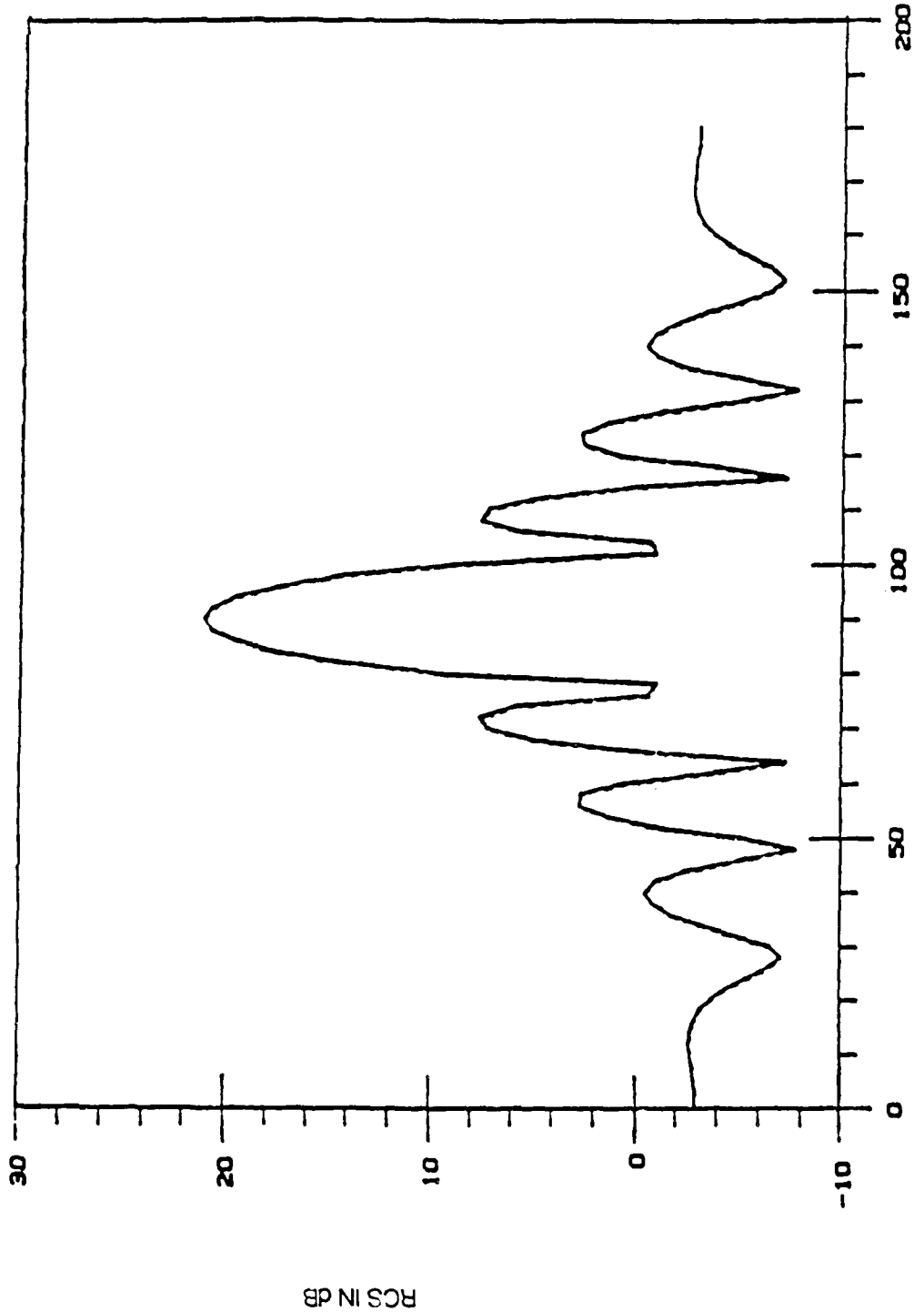

Figure 2.6 Bistatic RCS for normal incidence.
Solid line --- CGM.
Dotted line -- Preconditioning.

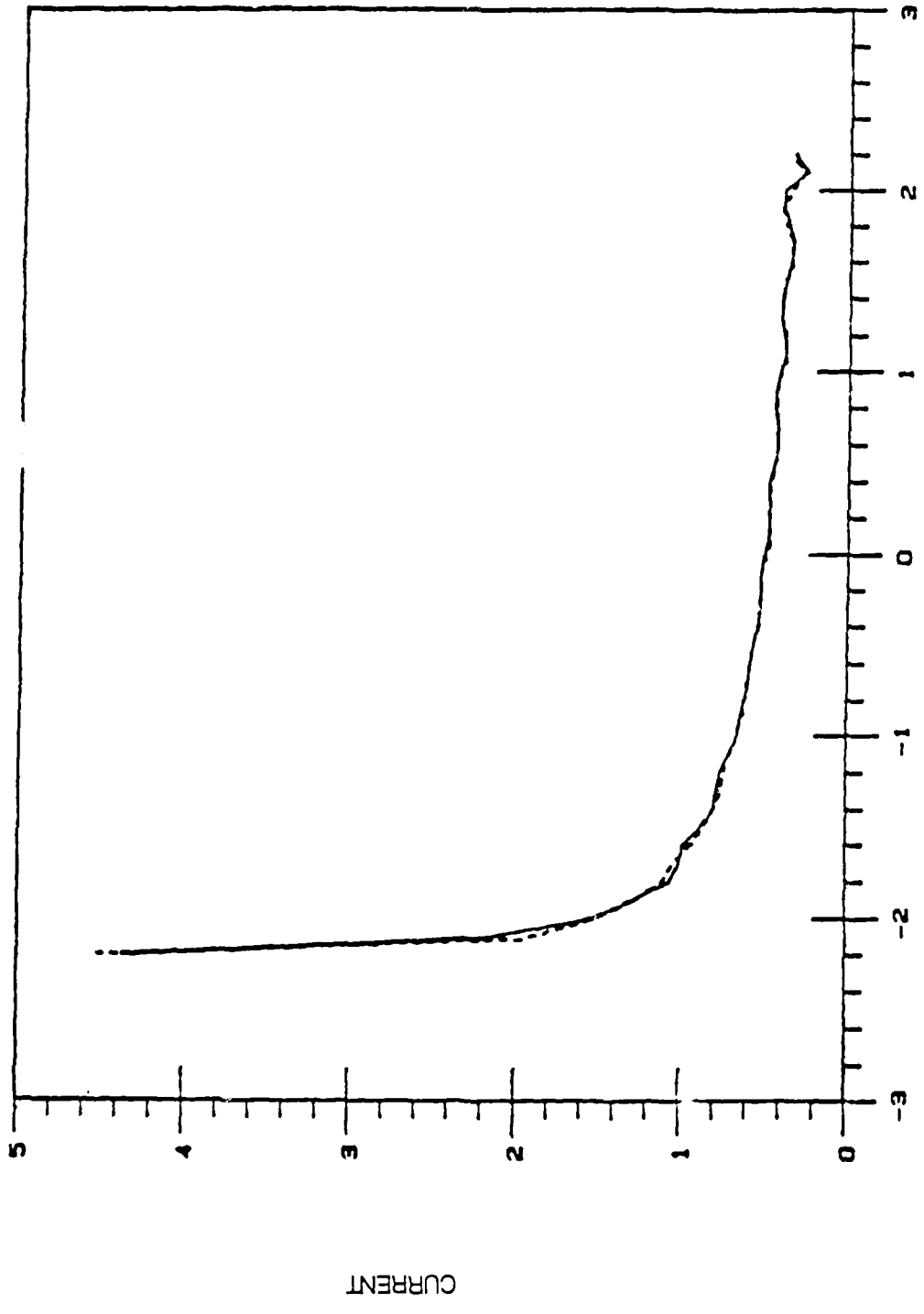

Figure 2.7 Magnitude of the induced current for grazing incidence.
Solid line --- CGM.
Dotted line -- Preconditioning.

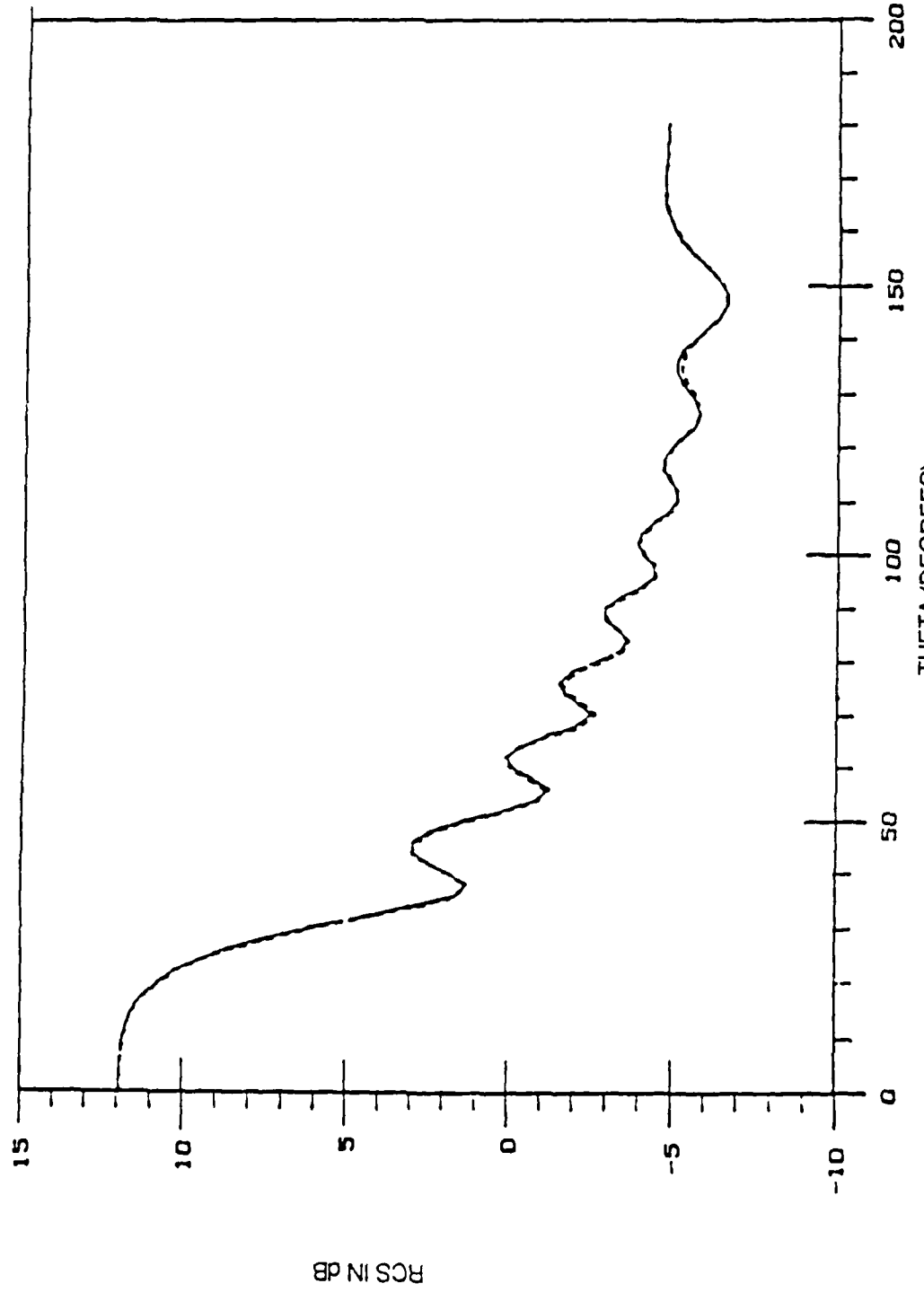

Figure 2.8 Bistatic RCS for grazing incidence.
Solid line --- CGM.
Dotted line -- Preconditioning.

2.5 Spectral Iterative Technique (SIT)

2.5.1 Conventional SIT

The spectral iterative technique has been applied to electromagnetic problems by a number of authors [12], [13], [14], [15], [16]. The conventional SIT algorithm can be derived for the edge-loaded strip case as follows. The integral equation in Eq. (2.40) can be rewritten as

$$\theta R(x)\, J(x) - \theta \int_{-\infty}^{\infty} J(x')\, G_p(x,x')\, dx' = \theta y(x) \quad \text{for all } x \tag{2.42}$$

where θ is the truncation factor mentioned before. Rearranging the above equation, we get

$$\theta R(x)\, J(x) - \theta y(x) + \hat{\theta} \int_{-\infty}^{\infty} J(x')\, G_p(x,x')\, dx' = \int_{-\infty}^{\infty} J(x') G_p(x,x')\, dx' \tag{2.43}$$

where $\hat{\theta}$ *is the complementary truncation factor which is* 0 *on the strip and* 1 otherwise. Since

$$\int_{-\infty}^{\infty} J(x')\, G_p(x, x')\, dx' = F^{-1}(JG_p) \tag{2.44}$$

we can write Eq. (2.43), after Fourier transforming it, as

$$JG_p = F\langle \theta R(x)\, J(x) - \theta y(x) + \hat{\theta} F^{-1}(JG_p) \rangle \tag{2.45}$$

From this equation we can get the iteration scheme

$$J_{n+1} = G_p^{-1}\, F\langle \theta R(x)\, J_n(x) - \theta y(x) + \hat{\theta}\, F^{-1}(J_n G_p) \rangle \tag{2.46}$$

This is the conventional SIT equation solving for the current induced on the strip. The success of this algorithm depends upon the assumption that J_{n+1}, computed from Eq. (2.46), represents a better approximation to the true solution than the previous iterate J_n. Notice that, if the strip is not perfectly conducting, then the inverse of G_p does not approximate too well the true inverse operator of the integral equation given in Eq. (2.42) and the solution does not necessarily improve with iteration. In fact, when R(x) exceeds a certain maximum value, the algorithm actually becomes unstable or divergent. However, for small values of R(x), SIT appears to work quite well because, as the resistivity on the strip is reduced to zero and the strip becomes perfectly conducting, the inverse of G_p does indeed approximate quite closely the true inverse of the original operator.

2.5.2 Modified SIT : SIT combined with SMS

The spectral iteration with the second minimization step is an attempt to improve the original SIT algorithm such that the procedure does not diverge even at its worst. Of course, this does not mean the algorithm will converge quickly. However, although the convergence may be slow in some cases, this combination guarantees that the algorithm will not diverge as in the case of the original SIT. The basic idea is to use the SIT equation to generate the g_n's, the current expansion functions, instead of generating the J_n's, the updated currents themselves. The equation for calculating the g_n's is given by

$$\text{new } g_n = G_p^{-1} \, F\!<\theta R(x)\, g_n(x) - \theta F_{n-1}(x) + \hat{\theta} F^{-1}(g_n\, G_p)> \tag{2.47}$$

where

$$F_n = y - L\, x_n \tag{2.48}$$

With the g_n's obtained from Eq. (2.47), we proceed to SMS to compute the appropriate η_n's, the weight coefficients, for these current expansion functions by minimizing the boundary condition error. Although improved in the sense that it does not diverge for all the values of resistivity, results show that the convergence of this modified SIT becomes slow when R(x) exceeds a certain maximum value.

2.6 Block iteration : A Hybrid Approach Based on a Combination of Iteration with MoM

To solve radar scattering problems for electrically large bodies by conventional methods requires large storage and computation times; these are major limiting factors in many cases. The block iteration approach is a scheme which attempts to circumvent these difficulties. The idea of block iteration is not new. In the past, however, the conventional block iteration had convergence problems, i.e.. the procedure diverged in many cases. In this section, it is shown that the block iteration can always be made nondivergent.

The block iteration is a scheme for solving a system of linear equations iteratively by scanning the matrix with a small window. It requires the matrix to be divided into small-order blocks, or windows, along the main diagonal. These windows are then solved in sequential manner, and the appropriate coefficients obtained by minimizing the boundary condition error are updated each time a window is solved. The advantage lies in the fact that the entire matrix need not be stored. At each step of the iteration procedure, only the window must be stored. The scheme is explained by the following simple example.

Suppose we have four prechosen basis functions g_1, g_2, g_3 and g_4. Given a problem of the type

$$L\,x = y \tag{2.49}$$

where L is a linear operator, y is a given excitation function, and x the unknown to be determined, we start the iteration procedure with an initial guess x_o obtained in a suitable manner. Typically

this initial guess is made by using, e.g., the physical optics approximation, or by simply choosing it equal to zero. Next, we redefine the unknown as the difference between the original unknown, x, and the initial guess, x_o, i.e.,

$$L\, x_1 = y - L\, x_o = y_1 \tag{2.50}$$

where x_1 is now the unknown to be determined, and solve Eq. (2.50) with the basis functions g_1 and g_2 by using the method of moments to obtain

$$x_1 = \eta_1^{(1)} g_1 + \eta_2^{(1)} g_2 \tag{2.51}$$

where the subscripts denote the corresponding basis functions and the superscript the stage of iteration. Using this x_1, we go through the usual SMS procedure outlined in Section 2.3.1 and calculate a weight coefficient $C^{(1)}$ which minimizes the error functional $| y_1 - Lx_1 |^2$. Using this weight coefficient, we write an improved solution to Eq. (2.50) as

$$x_1 = C^{(1)} (\eta_1^{(1)} g_1 + \eta_2^{(1)} g_2) \tag{2.52}$$

To proceed to the next stage of iteration, we again redefine our unknown, x_2, to be the difference between the original unknown, x, and the sum of x_o and x_1, and write

$$L\, x_2 = y - Lx_o - L\, x_1 = y - Lx_o - C^{(1)}(\eta_1^{(1)} Lg_1 + \eta_2^{(2)} Lg_2) = y_2 \tag{2.53}$$

By solving this equation with g2 and g3 and repeating the above procedure, we get

$$x_2 = C^{(2)} (\eta_2^{(2)} g_2 + \eta_3^{(2)} g_3) \tag{2.54}$$

This completes the second stage of the iteration. Finally, repeating the above procedure once more and adding an initial guess and those three "partial" solutions at each of the three iteration stages, we obtain the solution to the original equation

$$x = x_o + C^{(1)} \eta_1^{(1)} g_1 + (C^{(1)} \eta_2^{(1)} + C^{(2)} \eta_2^{(2)}) g_2$$

$$+ (C^{(2)} \eta_3^{(2)} + C^{(3)} \eta_3^{(3)}) g_3 + C^{(3)} \eta_4^{(3)} g_4 \qquad (2.55)$$

which is the desired solution obtained by the block iteration with the basis functions g_1 through g_4 and with the window size of two. In short, the block iteration is a scheme for generating appropriate expansion functions for the solution, the x_n's in the above example, by utilizing the method of moments and then improving the accuracy of the solution through the SMS procedure in a sequential manner. Each of these x_n's is a certain combination of the basis functions, g_n's, determined by the method of moments. Notice that if the g_n's are subdomain basis functions, then "uncoupling" between the matrix elements may occur and the block iteration achieves fast convergence. Howvever, if the g_n's are entire domain basis functions that are not well localized, as in the case of plane-wave-type basis functions, there is no uncoupling between the matrix elements, and the iteration procedure converges slower. Some results obtained by using the block iteration with the plane-wave-type basis functions show that this type of hybrid approach, where an iteration procedure is combined with the method of moments, is quite promising. As can be expected, the solution improves as the size of the window is increased.

2.7 Initial Guess

In using an iterative scheme, such as block iteration explained in the previous section, it is important to start the algorithm with a good initial guess if a rapid convergence is to be achieved. There may be several different ways of providing a reasonably good initial guesses for a particular

problem. In the following, we show some simple and inexpensive ways to generate reasonably good initial guesses by using the problem of scattering from edge-loaded strips as an example.

2.7.1 Angle-stepping

In the angle-stepping scheme, we first generate a good solution for one incident angle by using a numerically rigorous method, such as the method of moments or CGM, and then use that solution as an initial guess for another incident angle of interest. For example, a good solution for normal incidence may be generated and used as an initial guess for, say, 10 degrees off the normal incidence. The size of the angular increments can be varied to achieve the desired accuracy in the solution.

2.7.2 Physical optics

For resistively-loaded strips, the physical optics approximation implies the following :

$$J_o(x) = \begin{cases} \dfrac{E^{in}_{tan}(x)}{R(x)} & \text{if } R(x) \geq \dfrac{\eta}{2} \\ \\ 2\,\mathbf{n} \times \mathbf{H}^{in}(x) & \text{if } R(x) \leq \dfrac{\eta}{2} \end{cases} \tag{2.56}$$

where η is the intrinsic impedance of the free space and $\mathbf{n}$ the unit normal vector to the surface of the strip. The physical optics approximation provides a fairly good initial guess if the incident field on the strip is close to normal, and if the strip is perfectly conducting. However, when one of these conditions is not satisfied, the physical optics approximation is usually quite poor.

2.7.3 Use of adjoint operator

Another way of generating an initial guess of the edge-loaded strips is to make use of the adjoint operator. Given an operator equation

$$L\,x = y \tag{2.57}$$

we compute the initial guess to be

$$x_o = \eta_o\, L^A\, y \tag{2.58}$$

where L^A denotes the adjoint operator, y the given excitation function, and η_o a complex constant obtained as a result of minimizing the boundary condition error at the initial step of iteration. The effectiveness of this type of initial guess depends on how well the adjoint operator approximates the inverse operator for a given angle of incidence. For scattering from the edge-loaded strips, it has been found that this choice of initial guess is somewhat complementary to the physical optics approximation. That is, this method yields a relatively good initial guess if the angle of incidence is close to grazing and if the strip is heavily edge-loaded, i.e., R_{max} is very large. Figures 2.9 and 2.10 show that the adjoint operator L^A approximates the inverse operator L^{-1} quite closely for the grazing incidence case. The dotted line represents the solution obtained by $L^A y$. Notice that it differs from the rigorous solution generated by CGM by only a complex constant. When this complex constant is generated by minimizing the boundary condition error $| y - Lx_a |^2$ and multiplying by $L^A y$, the resultant curve closely approximates the solution by CGM as shown in the figures. The strip is 4.5 λ wide, with edge load width 1 λ from each edge, and with R_{max} equal to 200 ohms.

For all of the three different methods of generating an initial guess given above, the multiplication of a complex coefficient obtained as a result of minimizing the boundary condition error at the initial step of iteration will, in general, improve the initial guess. Also, when the restart of the iteration is used, multiplying the solution by the coefficient obtained from minimizing the

boundary condition error at the last stage of the previous set of iterations will improve the convergence of the algorithm.

2.7.4 Numerical results

The following figures show the effect of combining the block iteration with different types of initial guesses. The strip is 4.5 λ wide, the width of the edge load is 1 λ from each edge, and R_{max} is equal to 200 ohms. Figures 2.11 and 2.12 are obtained by block iteration using the PO approximation as an initial guess for the grazing incidence case. Figures 2.13 and 2.14 are the results for the grazing incidence case obtained by stepping from the solution for normal incidence generated by CGM to grazing incidence with an angular increment of 10 degrees. Notice the siginicant improvement achieved by stepping as compared to the case where the PO approximation is used as an initial guess.

The size of the angular increment and the range of stepping are two important factors in the scheme of angle-stepping as demonstrated in the following examples. The strip is 10.5 λ wide and perfectly conducting. Figure 2.15 shows the solution for the grazing incidence case obtained by MoM using twenty plane-wave-type basis functions. Notice that the MoM solution does not approximate too well the singular behavior of the current at the edges. Figure 2.16 shows the solution generated by block iteration by stepping from the CGM solution for the normal incidence case to grazing incidence with angular increments of 10 degrees. The number of the basis functions is kept constant at twenty. Notice the improvement achieved both in the current and in the far field. Figure 2.17 shows the results obtained by beginning with the CGM solution for 20 degrees off grazing and using angular increments of 5 degrees to step to the grazing incidence case. By reducing the angular increment and the range of stepping, a better improvement is achieved both in the current and in the far field. Finally, as shown in Figure 2.18, the agreement is very good when we begin with the 170 degree CGM solution and step to the grazing incidence with angular increments of 2 degrees.

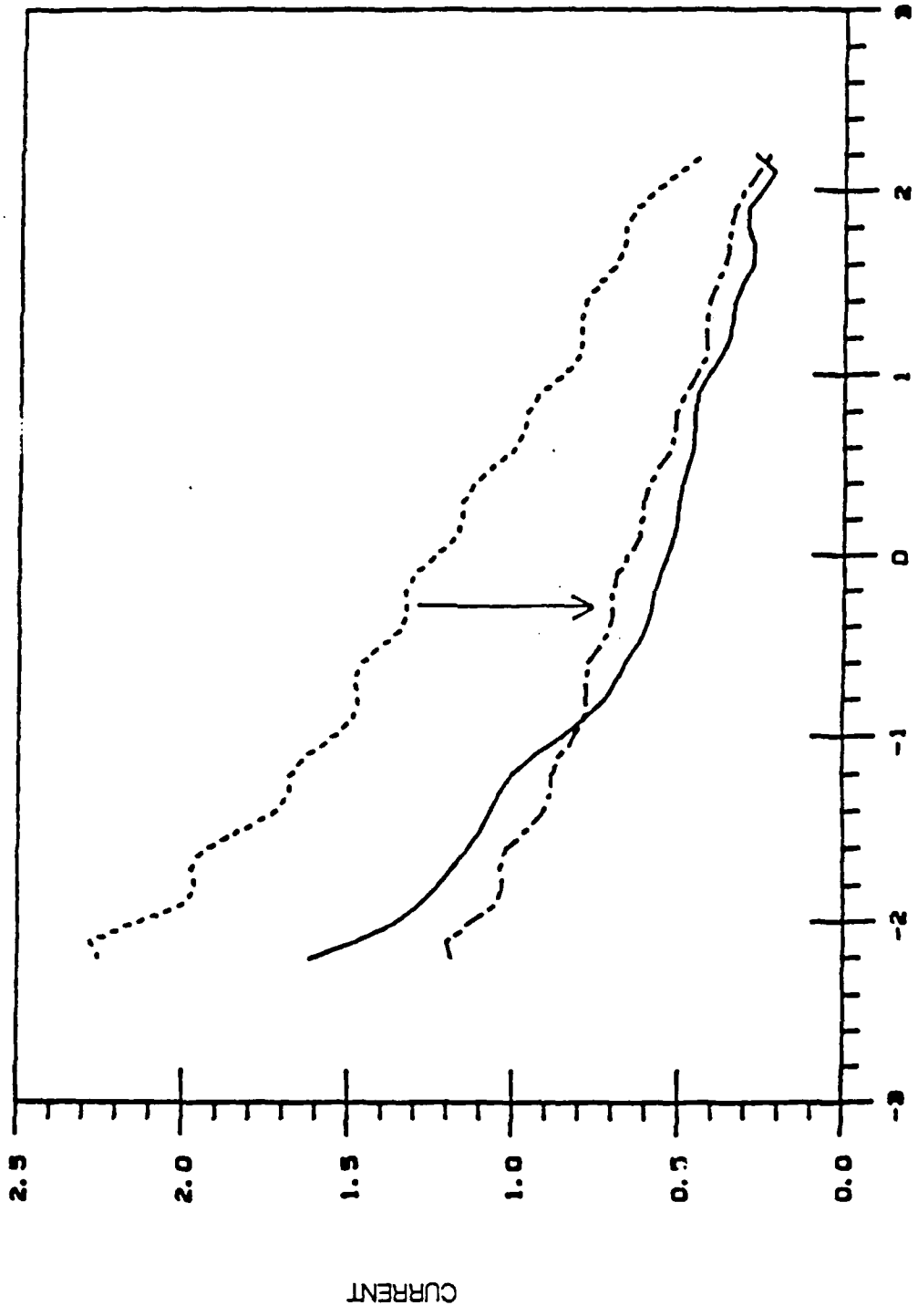

Figure 2.9 Magnitude of the induced current for grazing incidence.
Solid line --- CGM.
Dotted line -- Initial guess using the adjoint operator.

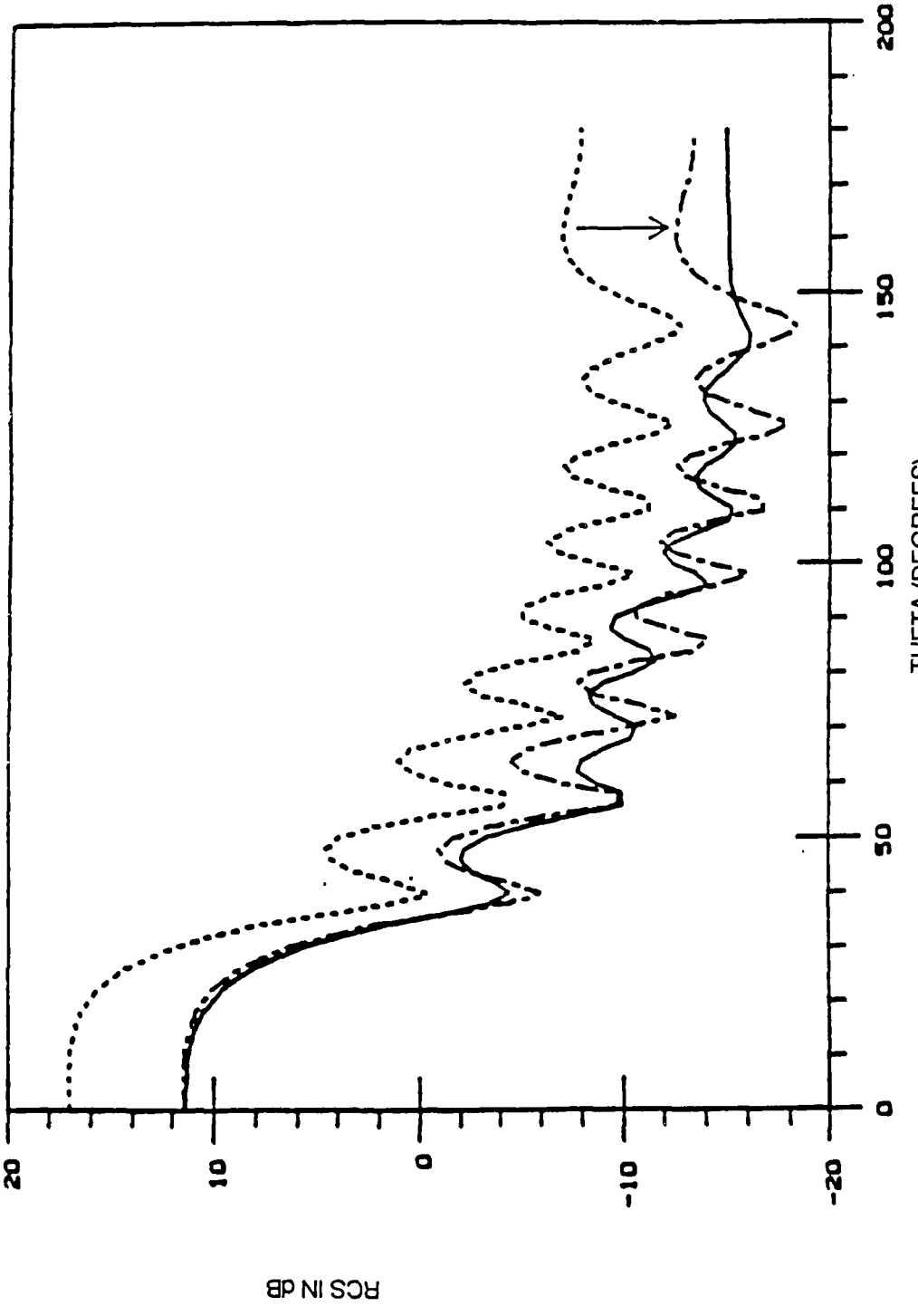

Figure 2.10 Bistatic RCS for grazing incidence.
Solid line --- CGM.
Dotted line -- Initial guess using the adjoint operator.

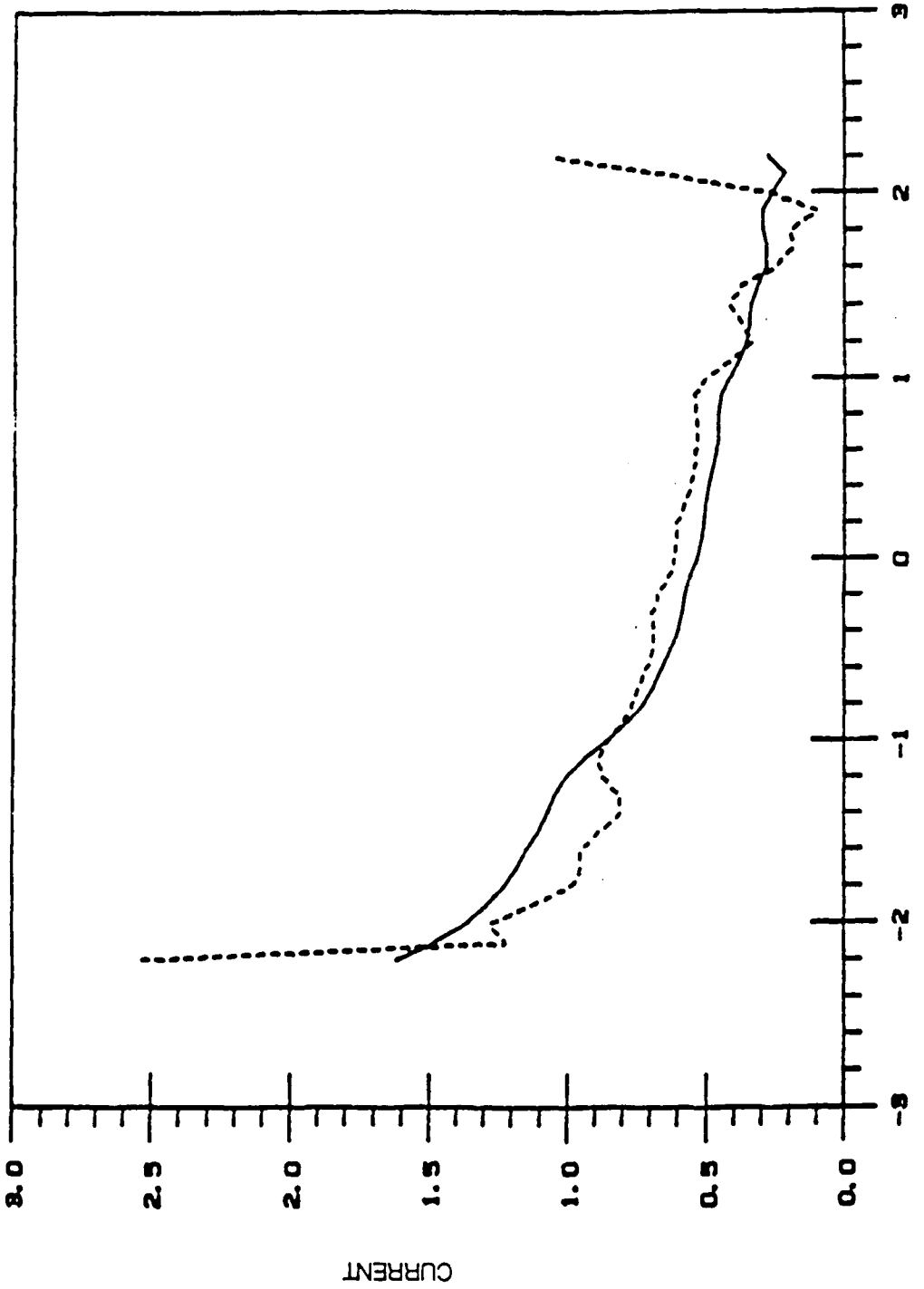

Figure 2.11 Magnitude of the induced current for grazing incidence.
Solid line --- CGM.
Dotted line -- Block iteration using 15 plane-wave-type functions with window size 5 and without stepping.

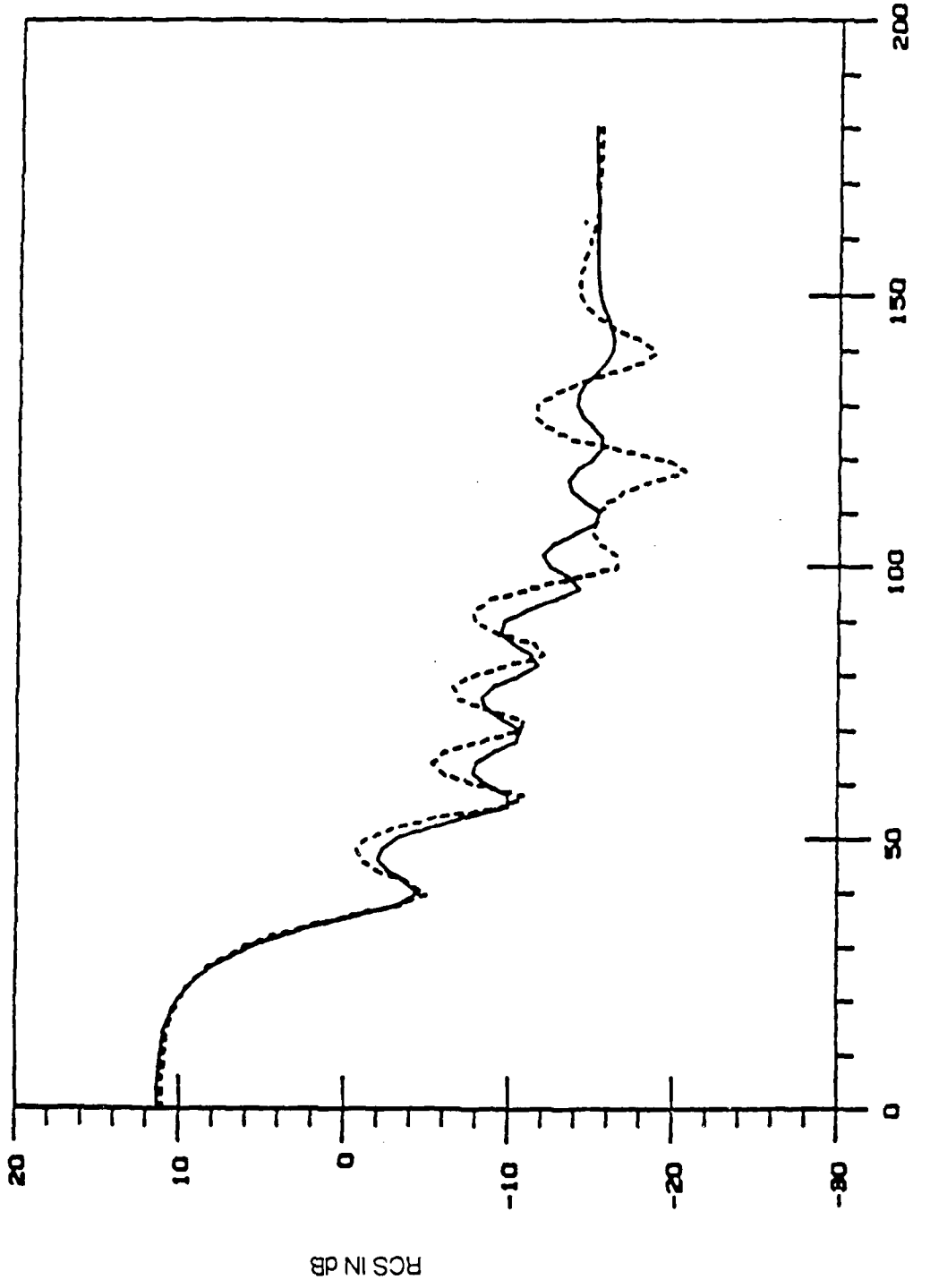

Figure 2.12 Bistatic RCS for grazing incidence.
Solid line --- CGM.
Dotted line -- Block iteration using 15 plane-wave-type functions with window size 5 and without stepping.

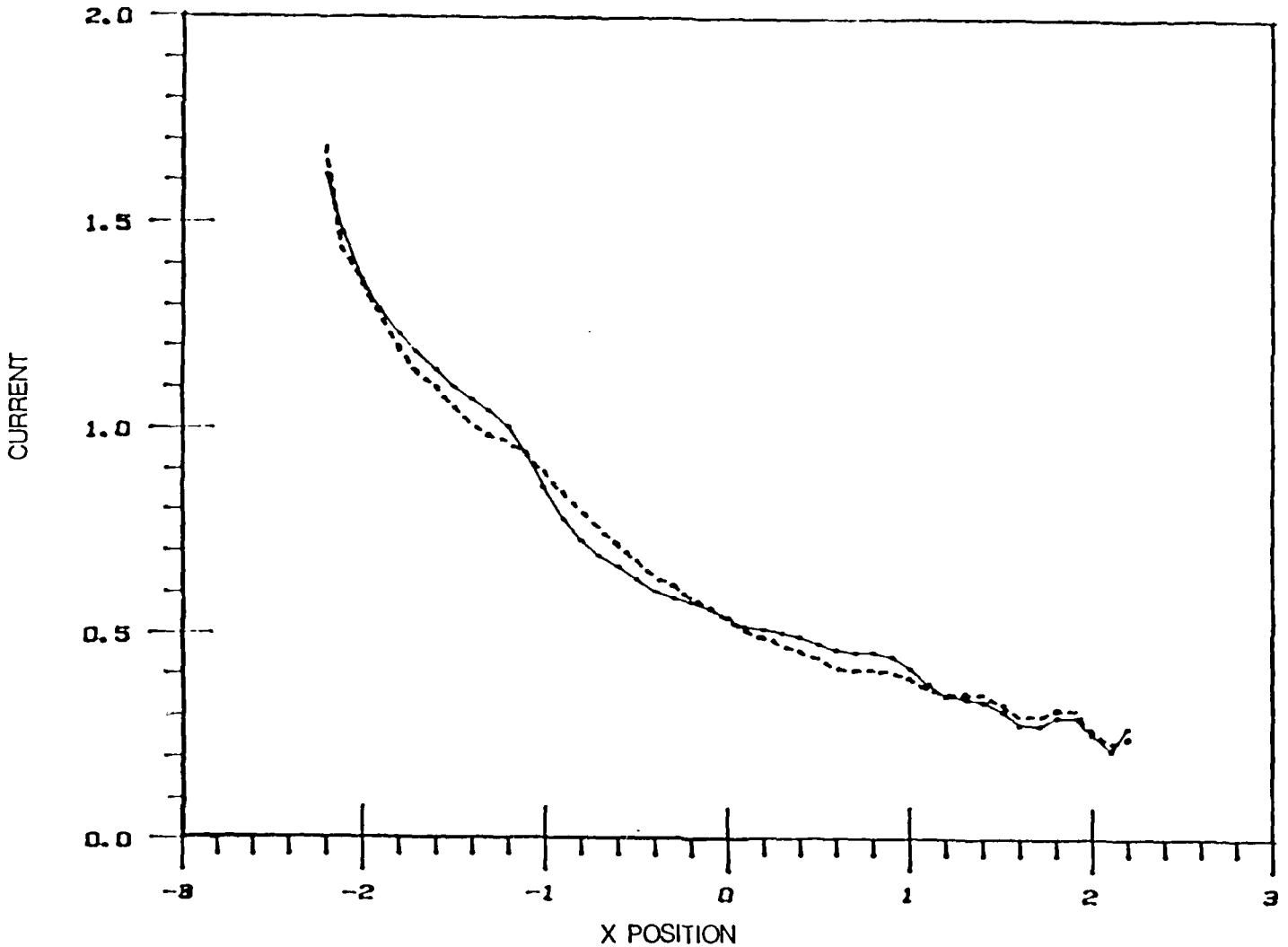

Figure 2.13 Magnitude of the induced current for grazing incidence.
Solid line --- CGM.
Dotted line -- Block iteration using 15 plane-wave-type functions with window size 5 and stepping from normal to grazing incidence with angular increment of 10 degrees.

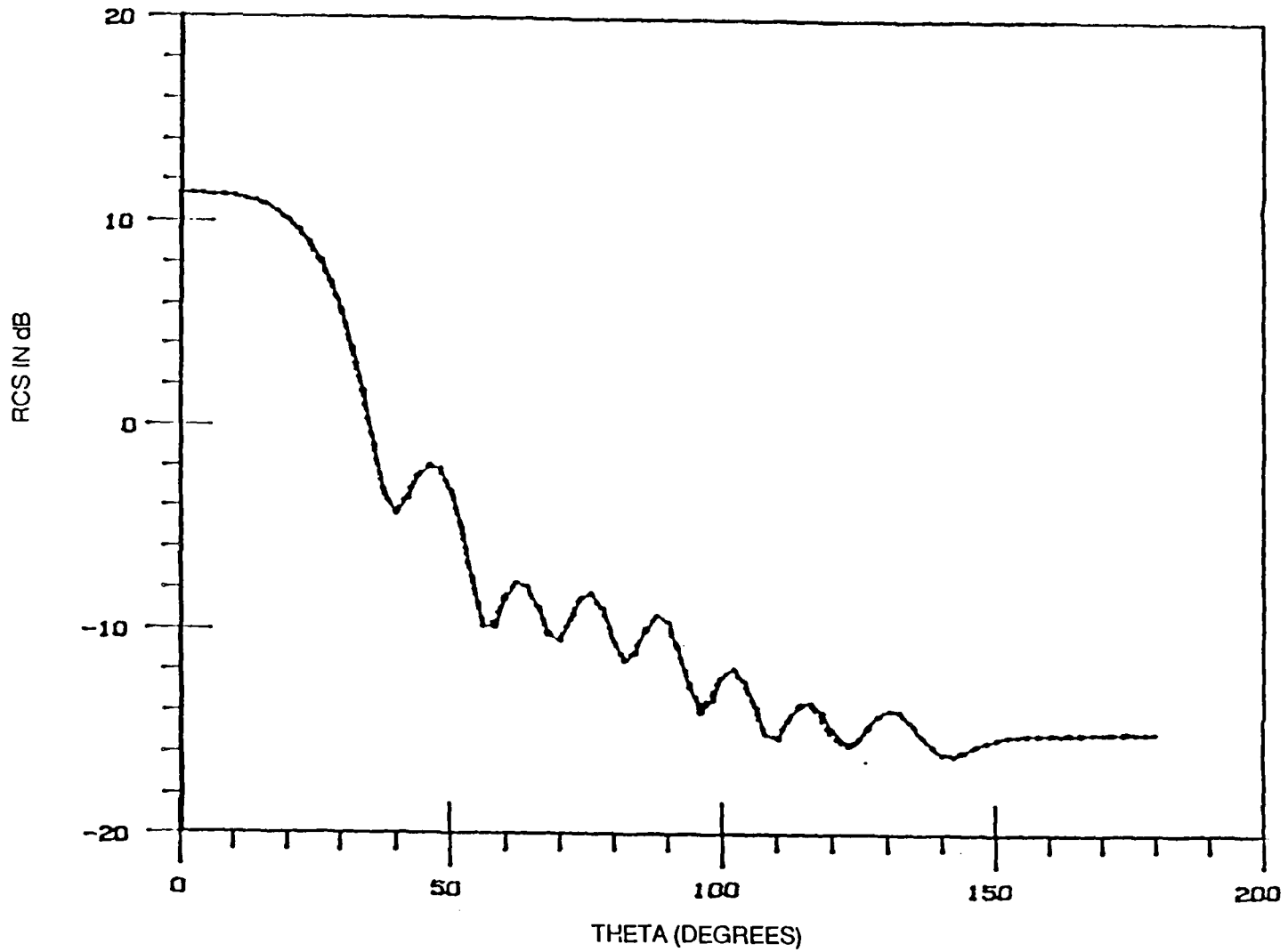

Figure 2.14 Bistatic RCS for grazing incidence.
Solid line --- CGM.
Dotted line -- Block iteration using 15 plane-wave-type functions with window size 5 and stepping from normal to grazing incidence with angular increment of 10 degrees.

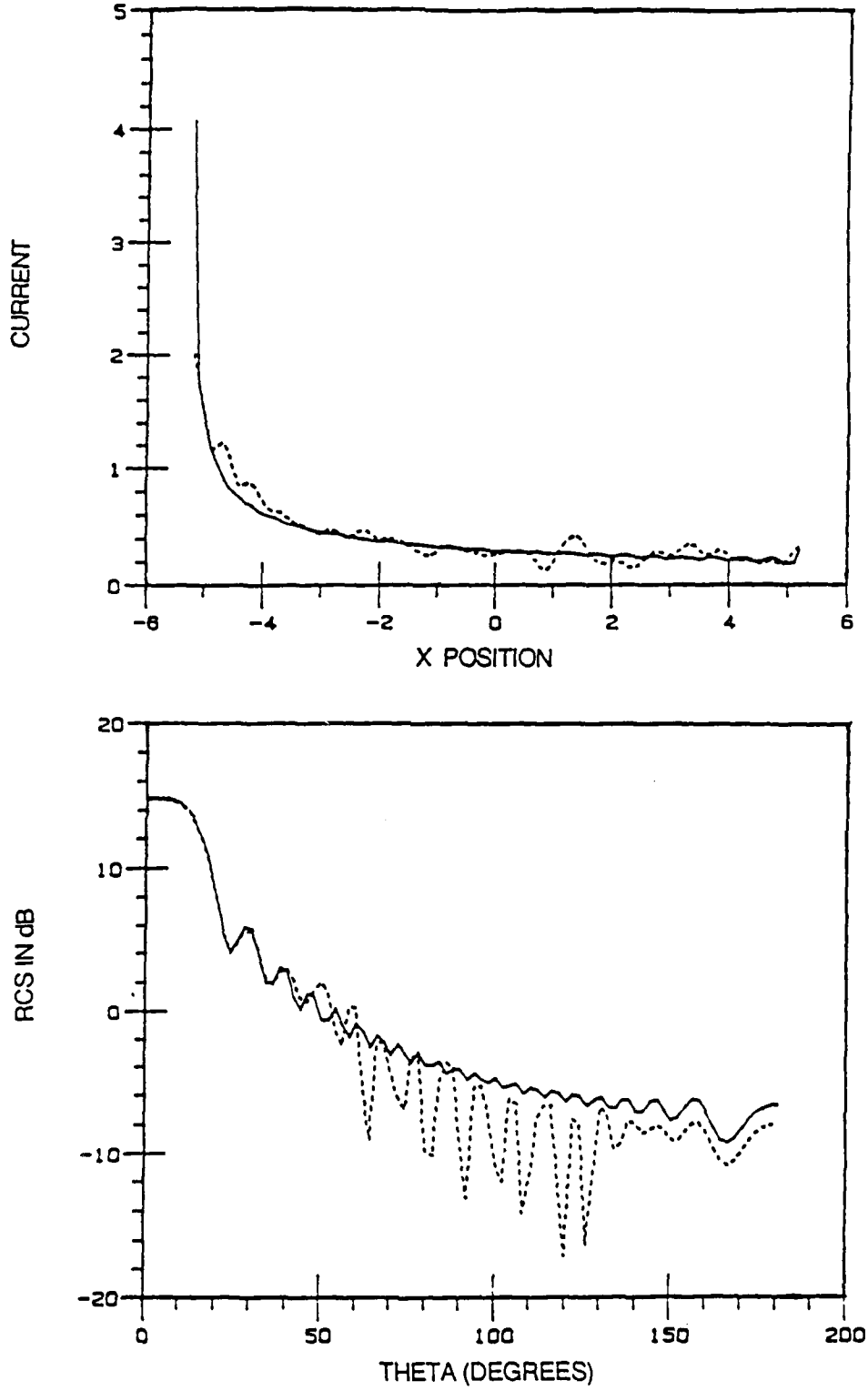

Figure 2.15 Top: Magnitude of the induced current for grazing incidence.
Bottom: Bistatic RCS for grazing incidence.
Solid line --- CGM.
Dotted line -- MoM using 20 plane-wave-type functions.

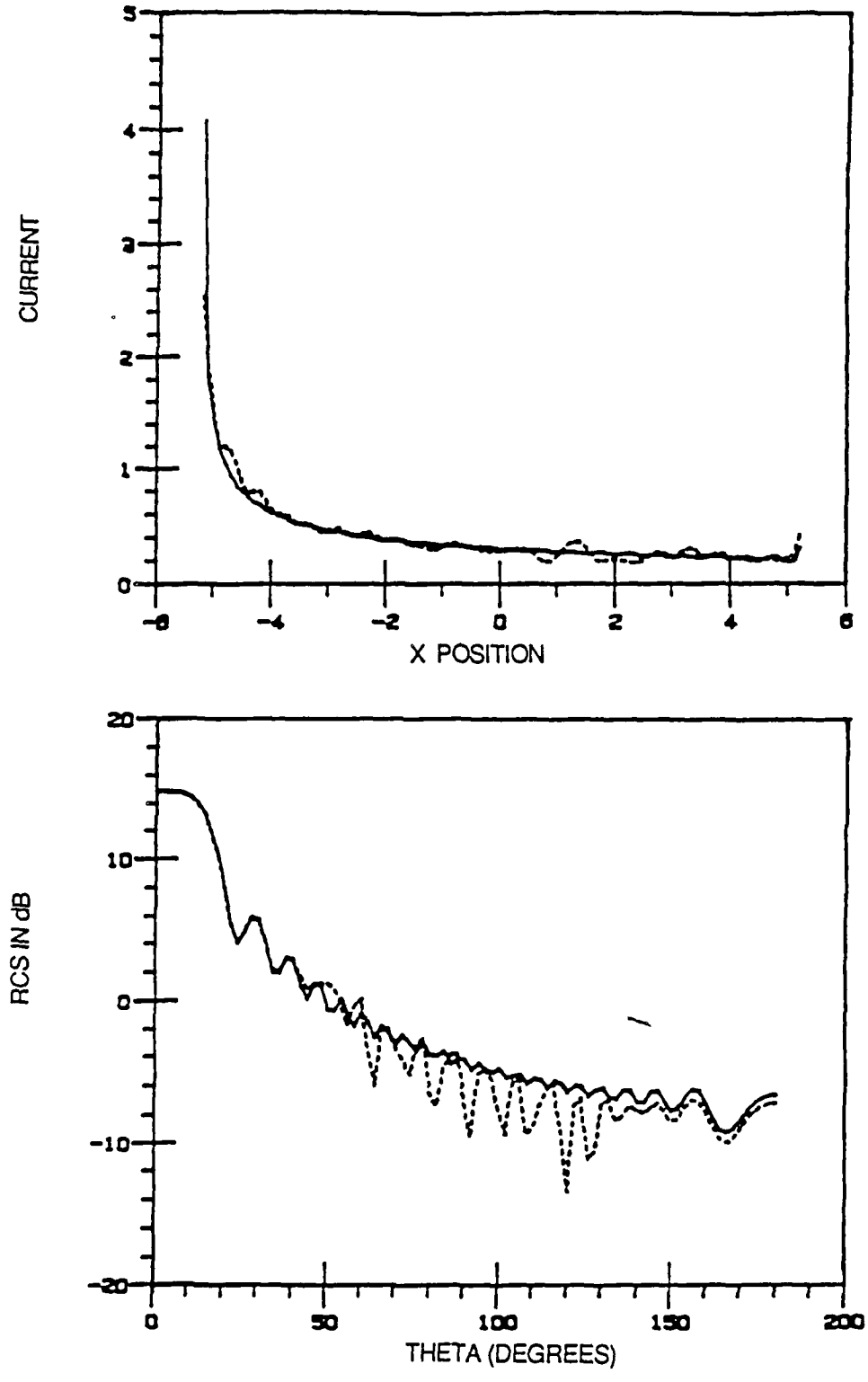

Figure 2.16 Top: Magnitude of the induced current for grazing incidence.
Bottom: Bistatic RCS for grazing incidence.
Solid line --- CGM.
Dotted line -- Block iteration using 20 plane-wave-type functions stepping from normal to grazing incidence with angular increment of 10 degrees.

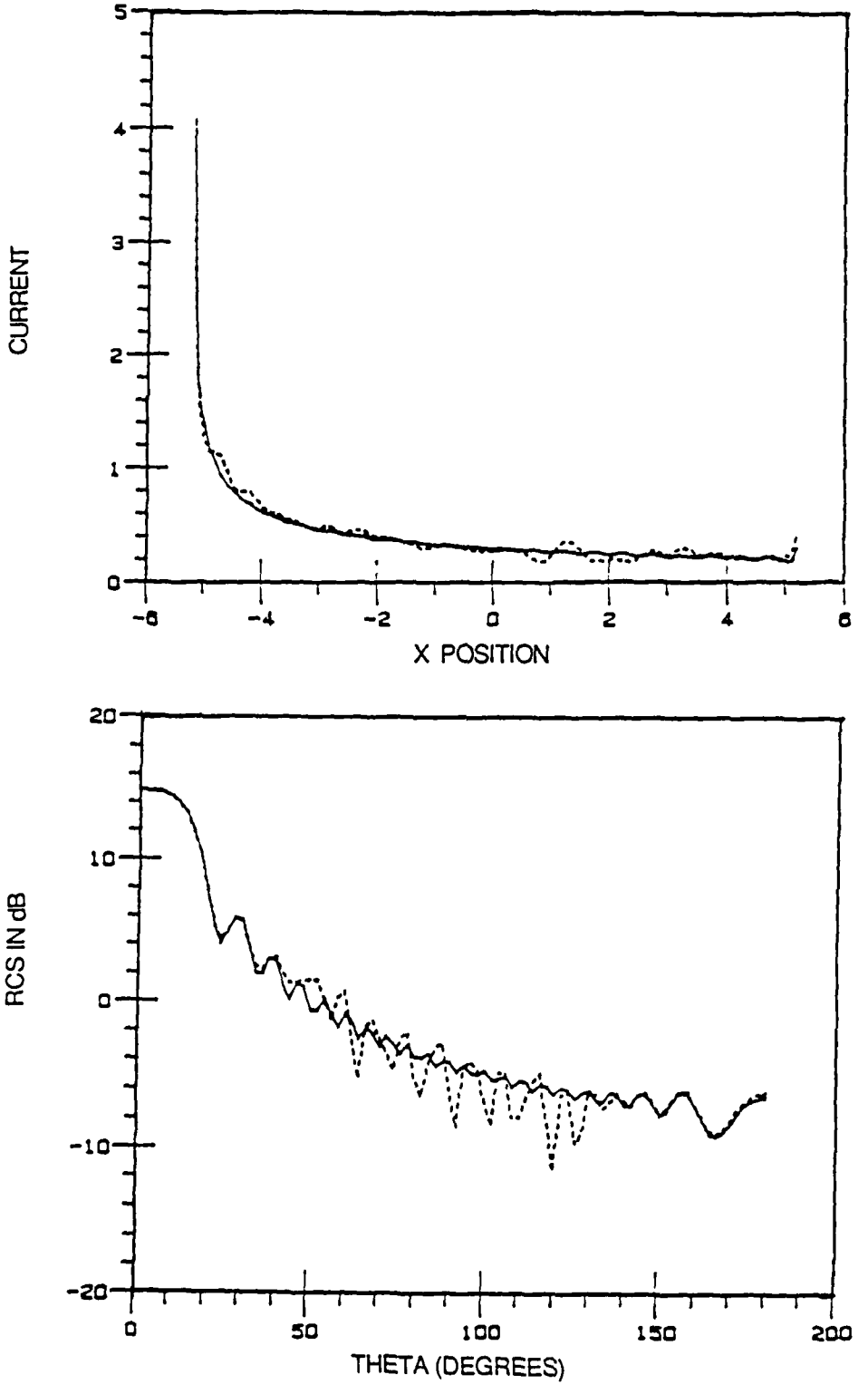

Figure 2.17 Top: Magnitude of the induced current for grazing incidence.
Bottom: Bistatic RCS for grazing incidence.
Solid line --- CGM.
Dotted line -- Block iteration using 20 plane-wave-type functions stepping from 160 degrees to grazing incidence with angular increment of 5 degrees.

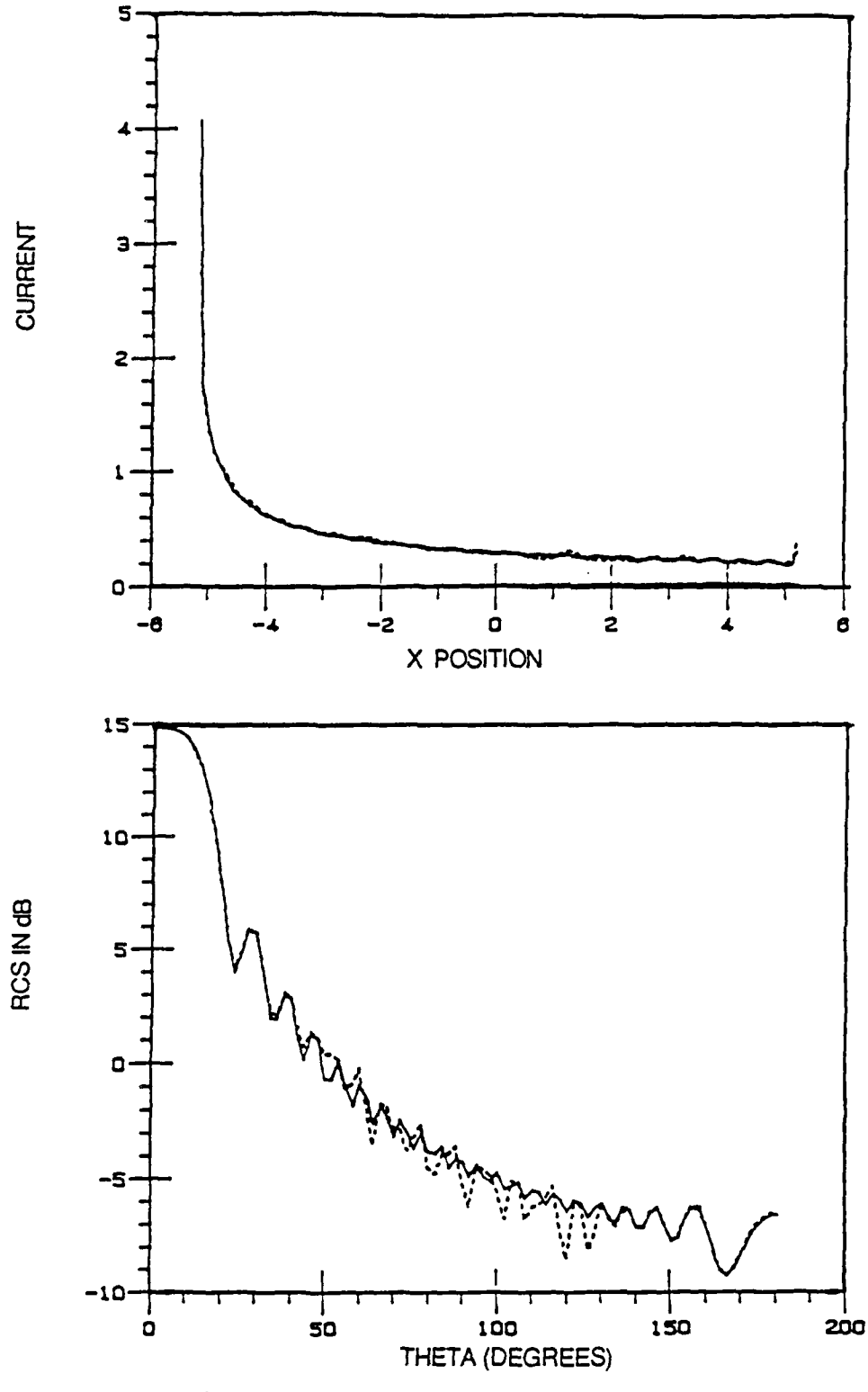

Figure 2.18 Top: Magnitude of the induced current for grazing incidence.
Bottom: Bistatic RCS for grazing incidence.
Solid line --- CGM.
Dotted line -- Block iteration using 20 plane-wave-type functions stepping from 170 degrees to grazing incidence with angular increment of 2 degrees.

The situation is similar for the case of edge-loaded strips, i.e., we can obtain better results by stepping in angle, just as in the case of PEC strips. We present the results for a 10.5 λ wide strip with the edge load width 1 λ from each edge and R_{max} equal to 200 ohms. Figures 2.19 and 2.20 show the MoM solution and the solution derived by stepping, respectively, with the latter obtained by starting with the normal incidence CGM solution and incrementally stepping all the way to the grazing incidence. It is especially worth noting that the disagreement between the current solutions at the edges of the strip, generated by CGM and MoM, is almost entirely eliminated when stepping is used.

2.8 Formulation for TE Scattering

The geometry of an edge-loaded strip and the coordinate system used for the TE case is shown in Figure 2.21. The incident fields are given by

$$\mathbf{H}^{in}(x,y) = \mathbf{z}\,\frac{e^{jk_o(x\cos\theta_o + y\sin\theta_o)}}{\eta} \tag{2.59}$$

$$\mathbf{E}^{in}(x,y) = (\,\mathbf{x}\,\sin\theta_o - \mathbf{y}\,\cos\theta_o\,)\,e^{jk_o(x\cos\theta_o + y\sin\theta_o)}$$

where θ_o is the incident angle measured from the positive x-axis and η the free-space wave impedance. For the TE polarization, only the x-component of the current on the strip is nonzero. When the general three-dimensional integral equation for a resistive scatterer is specialized to an infinitely thin resistive strip case, it becomes

$$E_x^{in}(x) = R(x)\,J_x(x) - E_x^{s}(x) \tag{2.60}$$

on the strip, where the incident field is given by

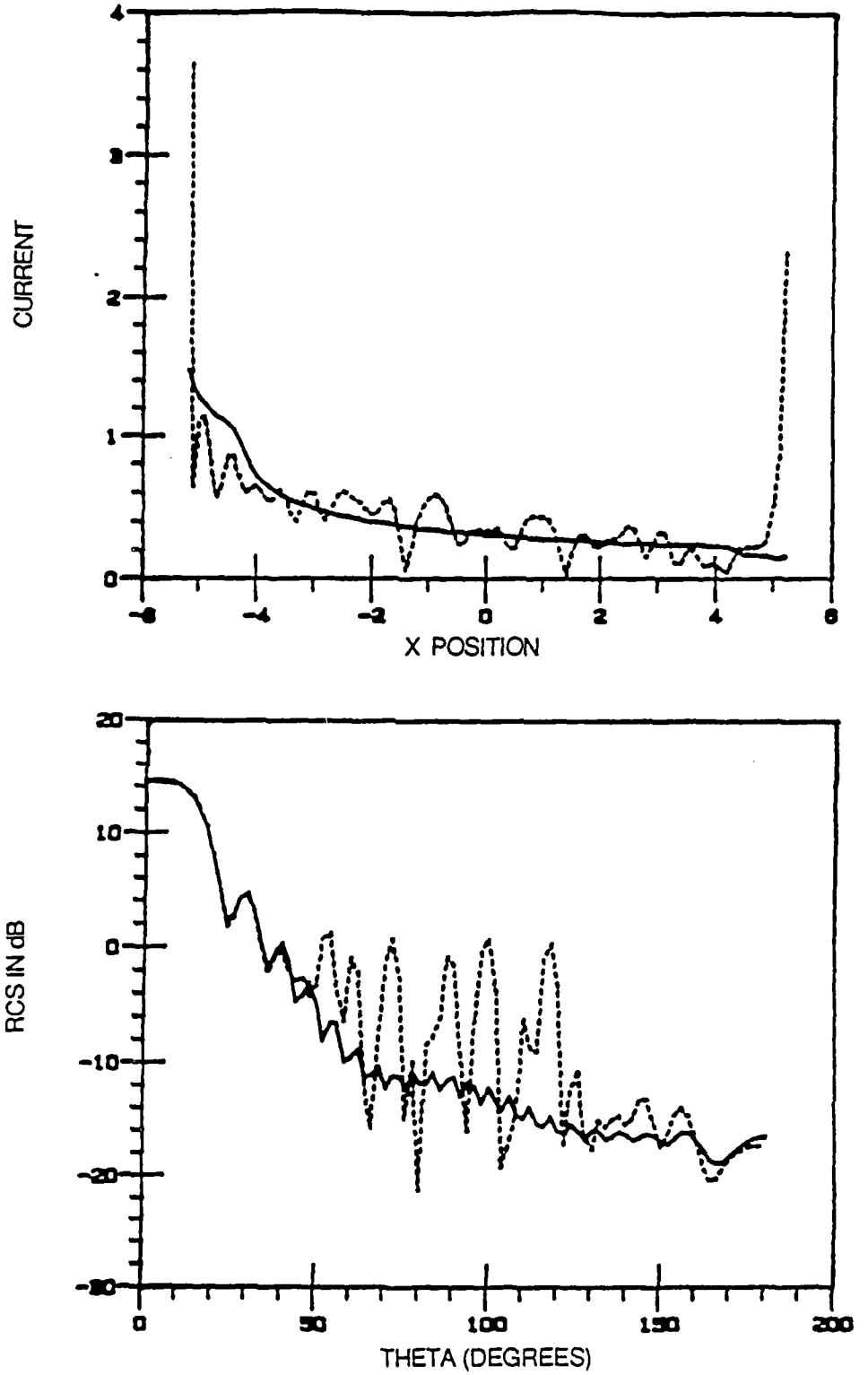

Figure 2.19 Top: Magnitude of the induced current for grazing incidence.
Bottom: Bistatic RCS for grazing incidence.
Solid line --- CGM.
Dotted line -- MoM using 20 plane-wave-type functions.

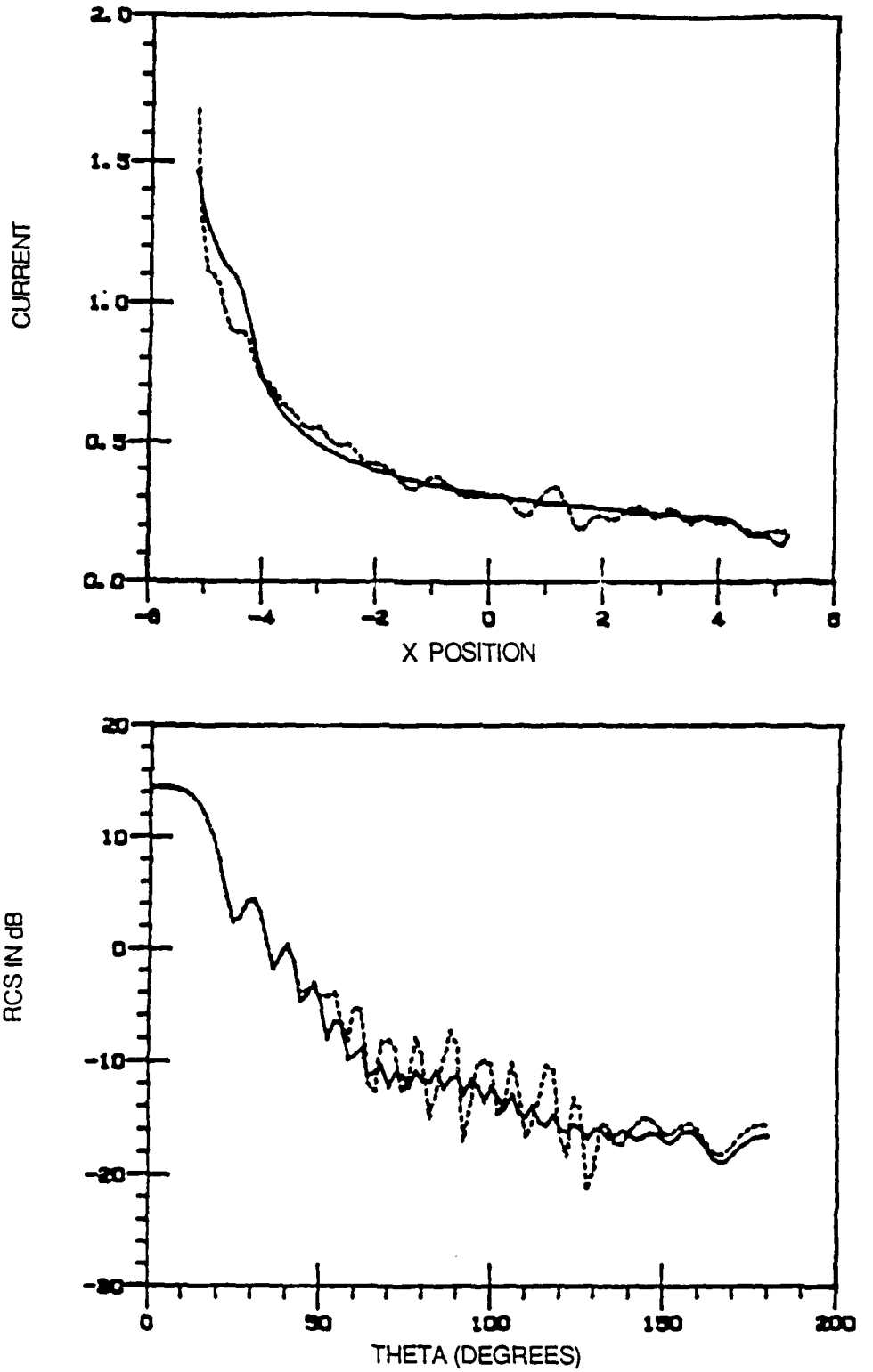

Figure 2.20 Top: Magnitude of the induced current for grazing incidence.
Bottom: Bistatic RCS for grazing incidence.
Solid line --- CGM.
Dotted line -- Block iteration using 20 plane-wave-type functions stepping from normal to grazing with angular increment of 10 degrees.

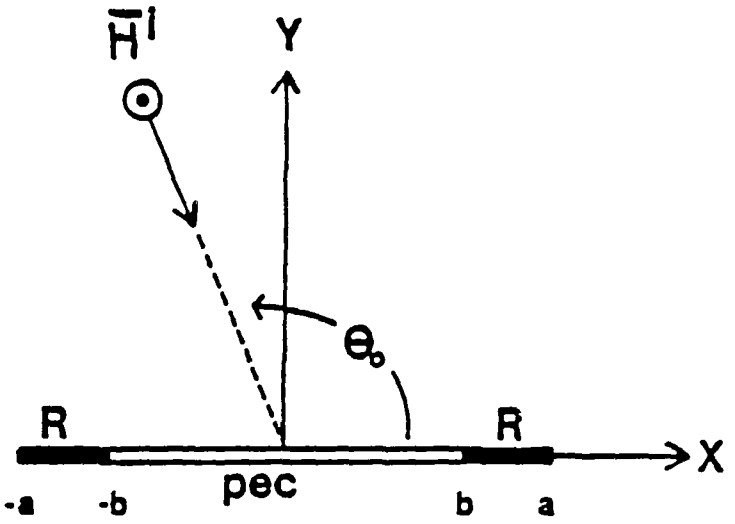

Figure 2.21 Geometry of the edge-loaded strip for TE scattering.

$$E_x^{in}(x) = \sin\theta_o \, e^{jk_o x\cos\theta_o} \tag{2.61}$$

The scattered field can be written as

$$E_x^s(x) = \frac{1}{j\omega\epsilon}\left(\frac{d^2}{dx^2} + k_o^2\right)\int_{-\infty}^{\infty} J_x(x')\, G(x,x')\, dx' \tag{2.62}$$

where k_o is the free-space wave number and G(x,x') is the two-dimensional Green's function given by

$$G(x,x') = \frac{1}{4j} H_o^{(2)}(k_o|x-x'|) \tag{2.63}$$

Fourier transforming both sides of Eq. (2.63), we have

$$E_x^s(\alpha) = \frac{1}{j\omega\epsilon}(k_o^2 - \alpha^2)\, J_x(\alpha)\, G(\alpha) = -\frac{\sqrt{k_o^2 - \alpha^2}}{2\omega\epsilon} J_x(\alpha) \tag{2.64}$$

where α is a spectral variable. By inverse Fourier transforming the right-hand side of Eq. (2.64), we obtain the scattered field in the space domain. All the techniques that are used to solve for TM scattering also apply to the TE case. In this section, only the results obtained from the conjugate gradient method and the block iteration using traveling waves as basis functions are shown as examples.

Figures 2.22 and 2.23 show the solutions for a 10.5 λ wide PEC strip obtained by MoM for the normal and 30 degrees above the grazing incident cases, respectively. Notice that, since MoM generates a fairly good solution with the allowed number of basis functions, the improvement in the solution, achieved by the process of stepping, is not as noticeable as in the case of TM strips (see Figure 2.24). Figures 2.25 and 2.26 show the results, obtained by MoM and by the stepping

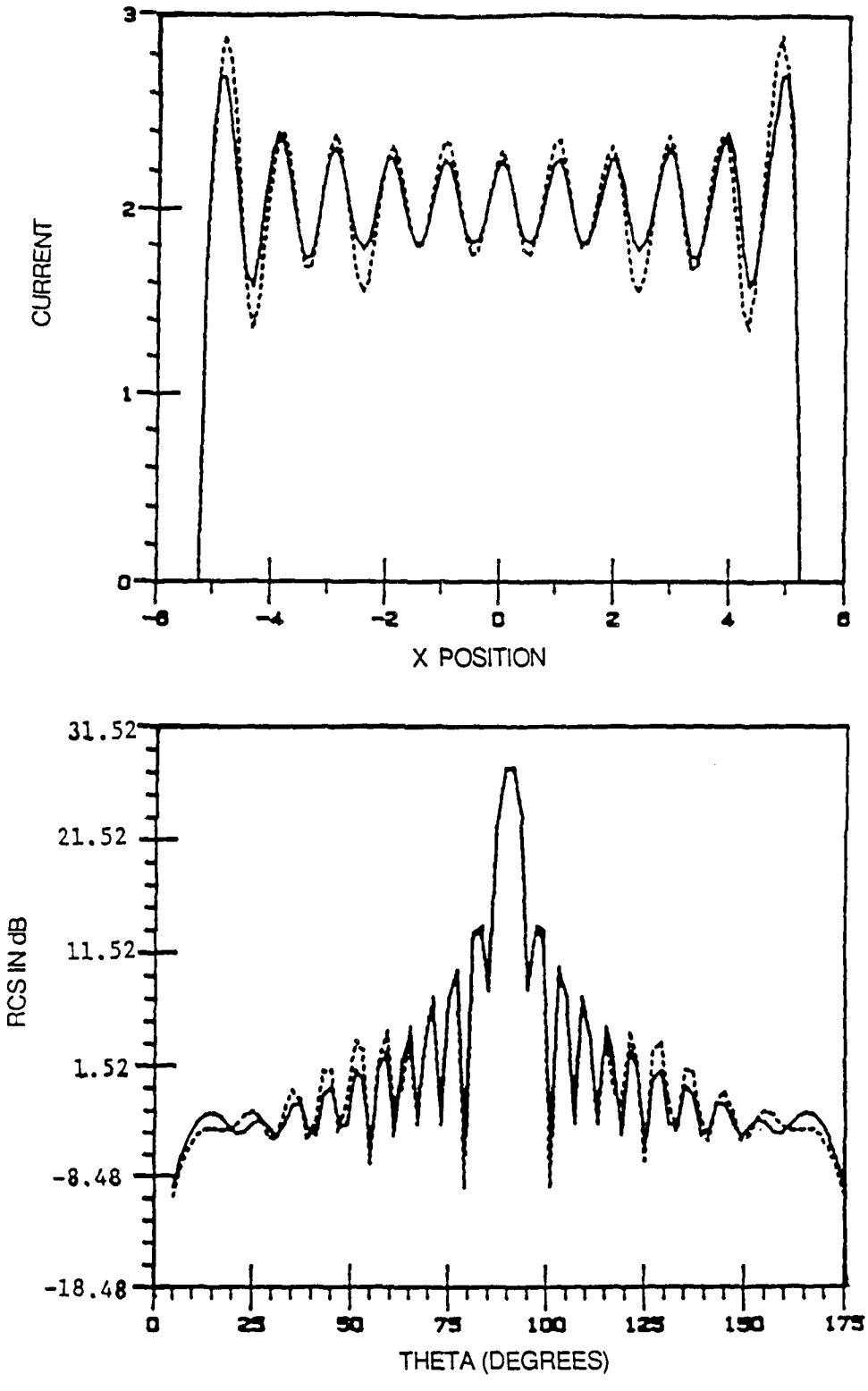

Figure 2.22 Top: Magnitude of the induced current for normal incidence.
Bottom: Bistatic RCS for normal incidence.
Solid line --- CGM.
Dotted line -- MoM using 20 plane-wave-type functions.

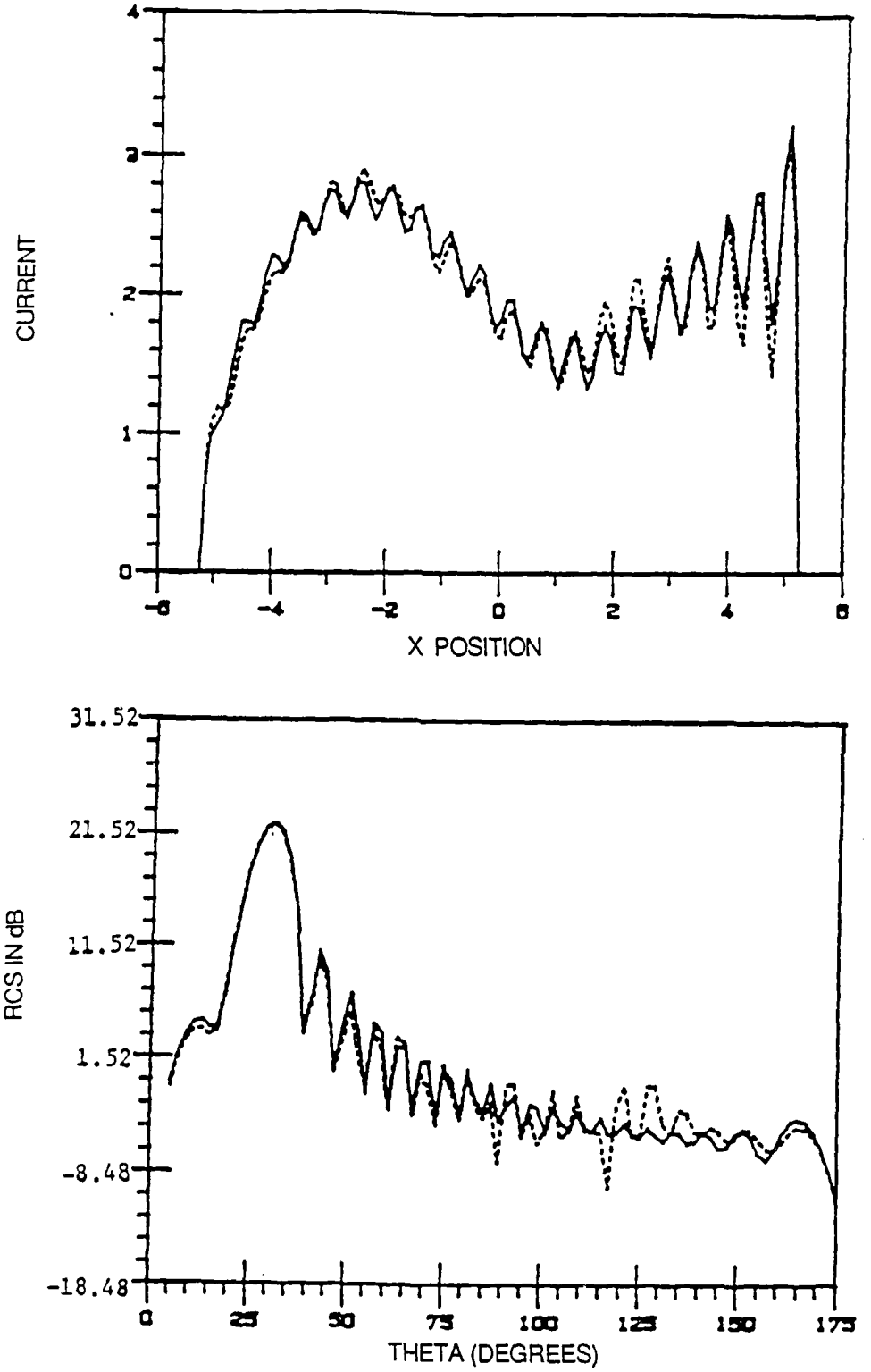

Figure 2.23 Top: Magnitude of the induced current for 150 degree incidence.
Bottom: Bistatic RCS for 150 degree incidence.
Solid line --- CGM.
Dotted line -- MoM using 20 plane-wave-type functions.

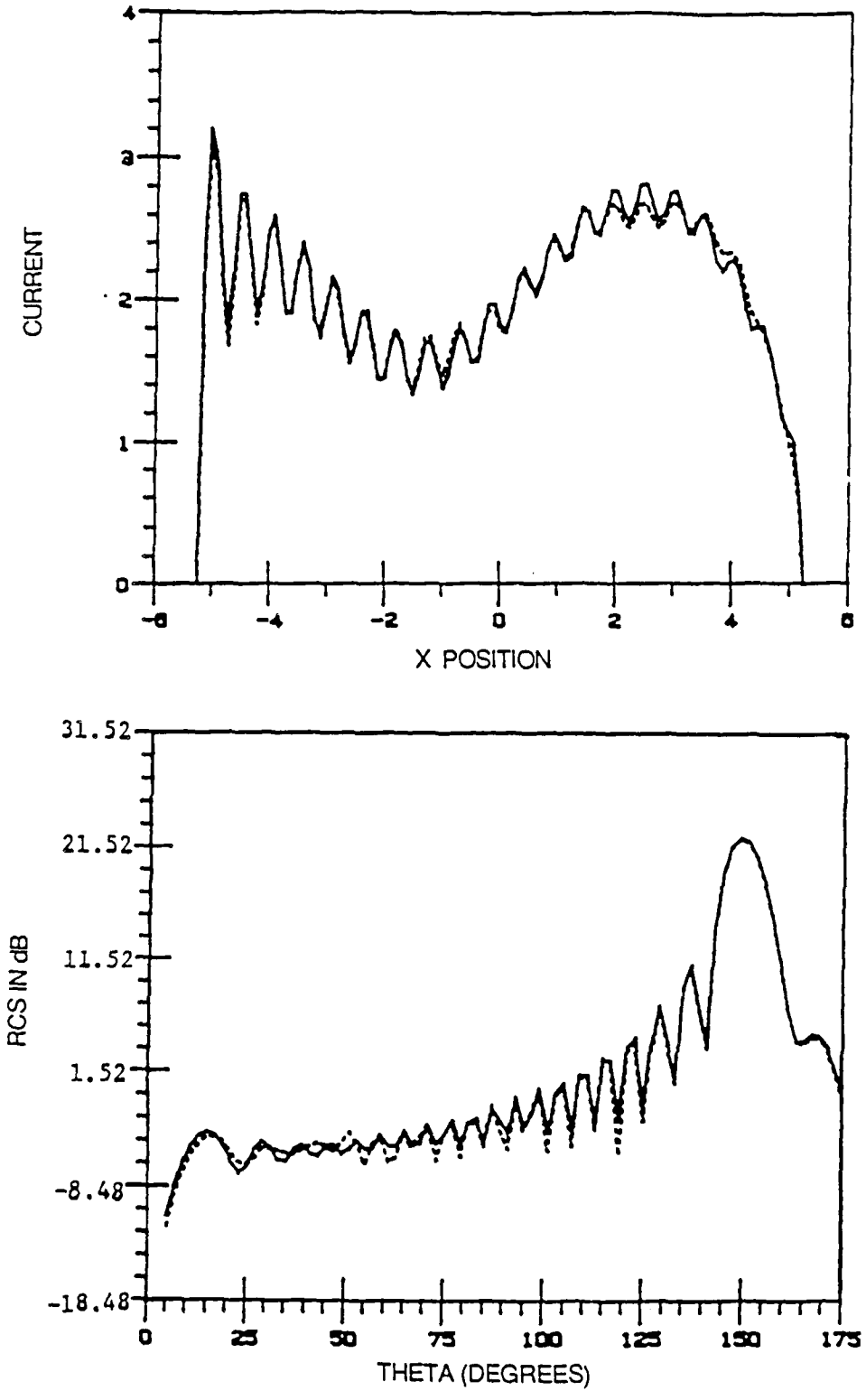

Figure 2.24 Top: Magnitude of the induced current for 30 degree incidence.
Bottom: Bistatic RCS for 30 degree incidence.
Solid line --- CGM.
Dotted line -- Block iteration using 20 plane-wave-type functions stepping from 50 to 30 degree incidence with angular increment of 5 degrees.

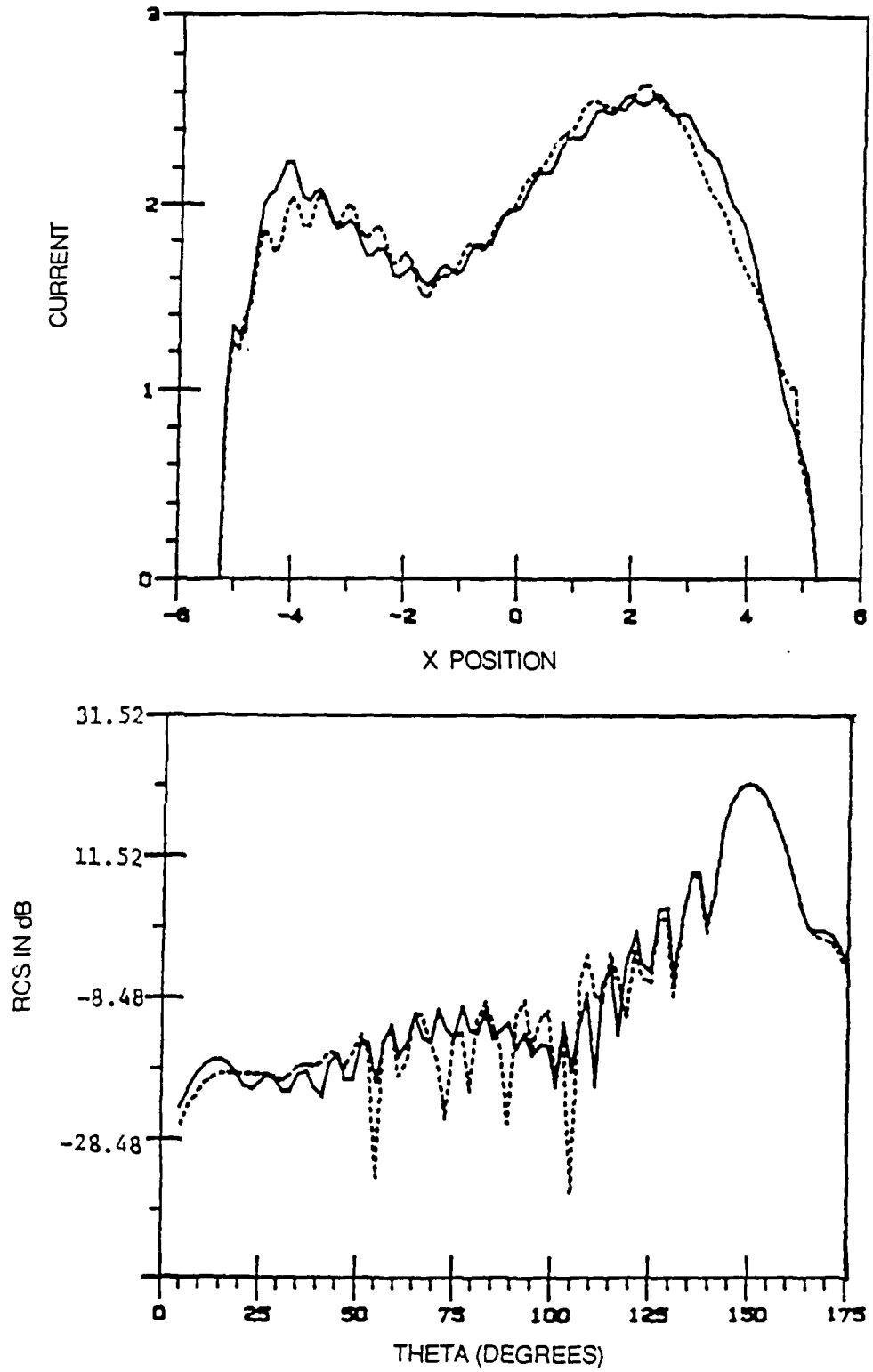

Figure 2.25 Top: Magnitude of the induced current for 30 degree incidence.
Bottom: Bistatic RCS for 30 degree incidence.
Solid line --- CGM.
Dotted line -- MoM using 20 plane-wave-type functions.

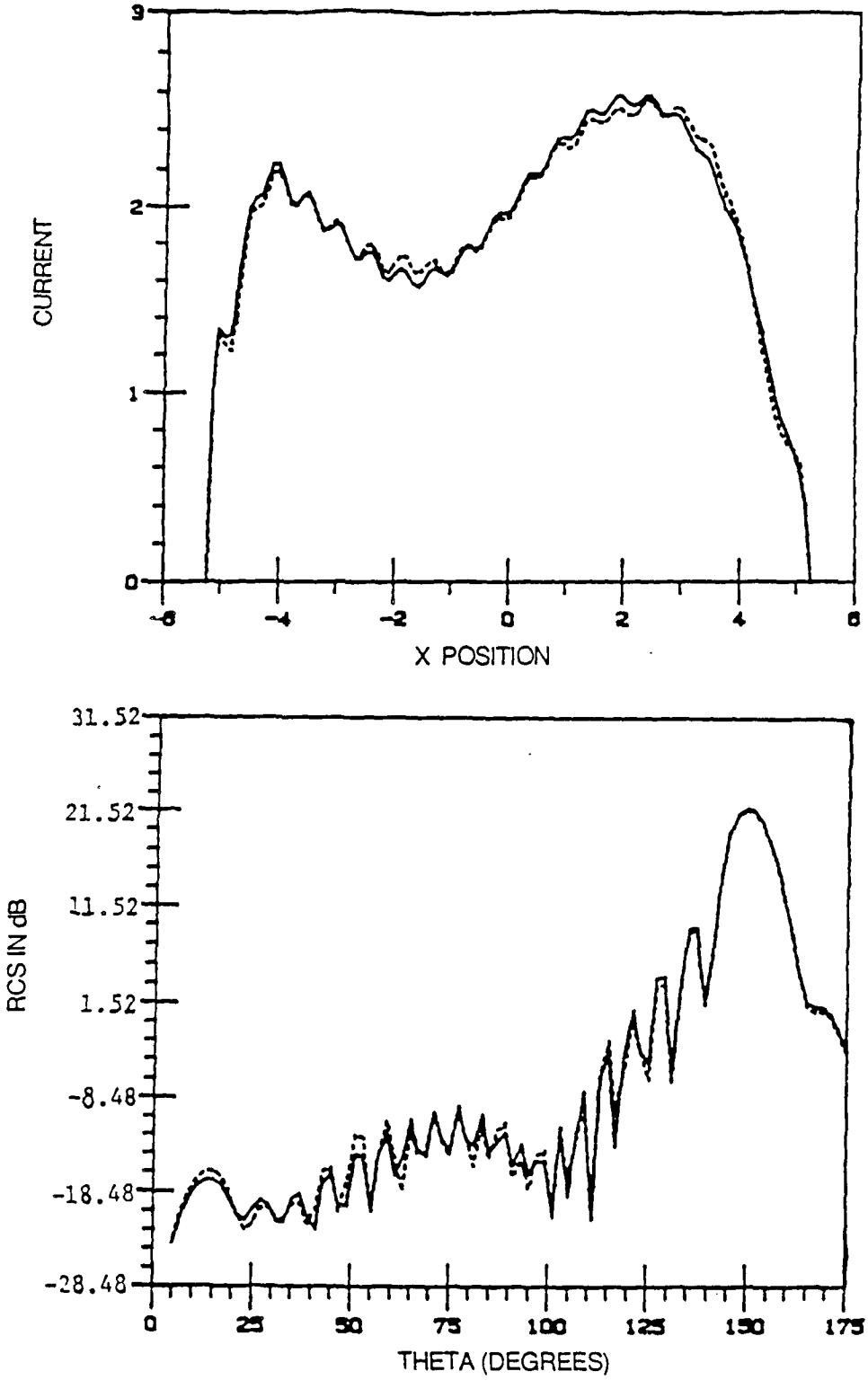

Figure 2.26 Top: Magnitude of the induced current for 30 degree incidence.
Bottom: Bistatic RCS for 30 degree incidence.
Solid line --- CGM.
Dotted line -- Block iteration using 20 plane-wave-type functions stepping from 50 to 30 degree incidence with angular increment of 5 degrees.

procedure, respectively, for a 10.5 λ wide edge-loaded strip with the edge load width 1 λ from each edge of the strip and R_{max} equal to 200 ohms. The improvement achieved by stepping is evident from the figures.

3. CONCLUSIONS

An alternative to directly inverting the large MoM matrix is to recast the problem into a form that is suitable for solution via iterative schemes. In this report, a number of iterative techniques that appear to be useful for solving the problem of electromagnetic scattering from electrically large bodies have been examined. It has been pointed out that, while the use of iterative methods may enable one to treat larger scatterers, most of them are not well-suited for handling multiple excitations in an efficient manner. Some variational-iteration schemes based on the use of prechosen entire domain basis functions that are suitable not only for treating larger bodies but for handling multiple incident angles as well have been suggested.

When compared to single-incidence oriented iterative algorithms, e.g., the conjugate gradient method, variational-iteration schemes seem to converge less rapidly. To enhance the computational efficiency of the variational-iteration methods, the scheme of angle-stepping, which provides better initial guesses, and the block-iteration approach, which is a hybrid method based on a combination of iteration with Mom, have been introduced. Some numerical examples have been given to demonstrate the effectiveness of the methods.

Although traveling-wave-type functions have been employed as basis functions in this report, the methods developed here can be applied equally well with any type of basis functions that can suitably represent the induced current on the scatterer. It is obvious that, for efficient computation, the functional form of the prechosen basis functions should be simple so that they can be easily implemented in the computer.

REFERENCES

[1] M. R. Hestenes and E. Stiefel, "Methods of conjugate gradients for solving linear systems," *J. Res. Nat. Bur. Stand.*, vol. 49, pp. 409-435, 1952.

[2] S. L. Ray and R. Mittra, "Spectral-iterative analysis of electromagnetic radiation and scattering problems," EM Report 84-11, University of Illinois, Urbana, 1984.

[3] A. F. Peterson and R. Mittra, "On the implementation and performance of iterative methods for computational electromagnetics," EM Report 85-9, University of Illinois, Urbana, 1985.

[4] M. Hurst and R. Mittra, "Scattering center analysis for radar cross-section modification," EM Report 84-12, University of Illinois, Urbana, 1984.

[5] P. M. Van den Berg, "Iterative computational techniques in scattering based upon the integrated square error criterion," *IEEE Trans. Antennas Propag.*, vol. AP-32, pp. 1063-1071, October 1984.

[6] T. K. Sakar, K. R. Siarkiewicz, and R. F. Stratton, "Survey of numerical methods for solution of large systems of linear equations for electromagnetic field problems," *IEEE Trans. Antennas Propag.*, vol. AP-29, pp. 847-856, November 1981.

[7] C. H. Chan, "Investigation of iterative and spectral Galerkin techniques for solving electromagnetic boundary value problems," Ph.D. dissertation, University of Illinois, Urbana, 1987.

[8] C. F. Smith, "The performance of preconditioned iterative methods in computational electromagnetics," Ph.D. dissertation, University of Illinois, Urbana, 1987.

[9] R. F. Harrington, Time-Harmonic Electromagnetic Fields. New York: McGraw-Hill, pp. 223-230, 1961.

[10] D. J. Evans (Ed.), Preconditioning methods: analysis and applications. New York: Gordon and Breach Science Publishers, 1983.

[11] G. H. Golub and C. F. Van Loan, Matrix Computations. Baltimore, Md. : The John Hopkins University Press, 1983.

[12] R. Kastner and R. Mittra, "Spectral-domain iterative techniques for analyzing electromagnetic scattering from arbitrary bodies," EM Report 82-1, University of Illinois, Urbana, 1982.

[13] W. L. Ko and R. Mittra, "A new approach based on a combination of integral equation and asymptotic techniques for solving electromagnetic scattering problems," *IEEE Trans. Antennas Propag.*, vol. AP-25, pp. 187-197, March 1977.

[14] R. Kastner and R. Mittra, "A spectral-iterative technique for analyzing scattering from arbitrary bodies, Part I : Cylindrical scatterers with E-wave incidence," *IEEE Trans. Antennas Propag.*, vol. AP-31, pp. 499-506, May 1983. "Part II : Conducting cylinders with H-wave incidence," *IEEE Trans. Antennas Propag.*, vol. AP-31, pp. 535-537, May 1983.

[15] R. Kastner and R. Mittra, "A new stacked two-dimensional spectral iterative technique (SIT) for analyzing microwave power deposition in biological media," *IEEE Trans. Microwave Theory Tech.*, vol. MTT-31, pp. 898-904, November 1983.

[16] C. H. Tsao and R. Mittra, "A spectral iteration approach for analyzing scattering from frequency selective surfaces," *IEEE Trans. Antennas Propag.*, vol. AP-30, pp. 303-308, March 1982.

END
DATE
10-88
DTIC